USAFSAM-TP-89-22

FEASIBILITY OF NMR DETECTION OF DECOMPRESSION BUBBLES

William L. Rollwitz

Southwest Research Institute
6220 Culebra Road
San Antonio, TX 78284

July 1990

Final Report for Period October 1985 - November 1987

Prepared for
USAF SCHOOL OF AEROSPACE MEDICINE
Human Systems Division (AFSC)
Brooks Air Force Base, TX 78235-5301

NOTICES

This final report was submitted by Southwest Research Institute, 6220 Culebra Road, San Antonio, Texas, under contract F33615-83-D-0602, job order 7930-18-5A, with the USAF School of Aerospace Medicine, Human Systems Division, AFSC, Brooks Air Force Base, Texas. Dr. Andrew A. Pilmanis and Captain Lauri L. Gordon (USAFSAM/VNBD) were the Laboratory Project Scientists-in-Charge.

Publication of this report does not constitute approval or disapproval of the ideas or findings. It is published in the interest of STINFO exchange.

When Government drawings, specifications, or other data are used for any purpose other than in connection with a definitely Government-related procurement, the United States Government incurs no responsibility or any obligation whatsoever. The fact that the Government may have formulated or in any way supplied the said drawings, specifications, or other data, is not to be regarded by implication, or otherwise in any manner construed, as licensing the holder, or any other person or corporation; or as conveying any rights or permission to manufacture, use, or sell any patented invention that may in any way be related thereto.

The Office of Public Affairs has reviewed this report, and it is releasable to the National Technical Information Service, where it will be available to the general public, including foreign nationals.

This report has been reviewed and is approved for publication.

Andrew A. Pilmanis

ANDREW A. PILMANIS, Ph.D.
Project Scientist

William F. Storm

WILLIAM F. STORM, Ph.D.
Supervisor

George Schwender MD

GEORGE E. SCHWENDER, Colonel, USAF, MC, CFS
Commander

UNCLASSIFIED

SECURITY CLASSIFICATION OF THIS PAGE

REPORT DOCUMENTATION PAGE

Form Approved OMB No. 0704-0188

1a. REPORT SECURITY CLASSIFICATION Unclassified	1b. RESTRICTIVE MARKINGS
2a. SECURITY CLASSIFICATION AUTHORITY	3. DISTRIBUTION/AVAILABILITY OF REPORT Approved for public release; distribution is unlimited.
2b. DECLASSIFICATION/DOWNGRADING SCHEDULE	
4. PERFORMING ORGANIZATION REPORT NUMBER(S) SwRI-15-8846	5. MONITORING ORGANIZATION REPORT NUMBER(S) USAFSAM-TP-89-22
6a. NAME OF PERFORMING ORGANIZATION Southwest Research Institute 6b. OFFICE SYMBOL (If applicable)	7a. NAME OF MONITORING ORGANIZATION USAF School of Aerospace Medicine (VNBD)
6c. ADDRESS (City, State, and ZIP Code) 6220 Culebra Road P. O. Box 28510 San Antonio TX 78284	7b. ADDRESS (City, State, and ZIP Code) Human Systems Division (AFSC) Brooks AFB TX 78235-5301
8a. NAME OF FUNDING/SPONSORING ORGANIZATION 8b OFFICE SYMBOL (If applicable)	9. PROCUREMENT INSTRUMENT IDENTIFICATION NUMBER F33615-83-D-0602
8c. ADDRESS (City, State, and ZIP Code)	10. SOURCE OF FUNDING NUMBERS PROGRAM ELEMENT NO. 61101F; PROJECT NO. 7930; TASK NO 18; WORK UNIT ACCESSION NO. 5A

11. TITLE (Include Security Classification)

Feasibility of NMR Detection of Decompression Bubbles

12. PERSONAL AUTHOR(S)

Rollwitz, William L.

13a. TYPE OF REPORT	13b. TIME COVERED	14. DATE OF REPORT (Year, Month, Day)	15. PAGE COUNT
Final	FROM 85/10 TO 87/11	1990, July	61

16. SUPPLEMENTARY NOTATION

17. COSATI CODES			18. SUBJECT TERMS (Continue on reverse if necessary and identify by block number)
FIELD	GROUP	SUB-GROUP	
20	05		
06	04		NMR, Blood, Decompression Bubbles, Detection

19. ABSTRACT (Continue on reverse if necessary and identify by block number)

The reported program had four tasks: (1) construct the bubble generator and modify the NMR equipment to contain it; (2) make the NMR measurements and determine $T_{11}^{\frown}$, $T_{12}^{\frown}$, and $T_2^{\frown}$ in blood samples both with and without bubbles of oxygen, air, and nitrogen; and (3) obtain a magnetic resonance image (MRI) of the knee and calculate the values of $T_1^{\frown}$ and $T_2^{\frown}$ in the synovial fluid in the knee and (4) final report. All of these tasks were completed. The bubble generator and the equipment modifications were made, tested successfully, and used to make two sets of NMR measurements on 25 samples of blood, in one sample of plasma and in two samples of water. Each sample had one of the following conditions: oxygen tonometer, oxygen bubbles, air tonometer, air bubbles, nitrogen tonometer, or nitrogen bubbles. In addition, some NMR measurements were made with flowing bubbles. From the NMR data, the relaxation times $T_2^{\frown}$, $T_{11}^{\frown}$, and $T_{12}^{\frown}$ were calculated. Two references were found which reported data that showed that the value of T_2 varied directly with the percent oxyhemoglobin and this condition was verified by the NMR measurements. The values of T_2 were the longest for

20. DISTRIBUTION/AVAILABILITY OF ABSTRACT	21. ABSTRACT SECURITY CLASSIFICATION	
☒ UNCLASSIFIED/UNLIMITED ☐ SAME AS RPT. ☐ DTIC USERS	Unclassified	
22a. NAME OF RESPONSIBLE INDIVIDUAL Andrew A. Pilmanis	22b. TELEPHONE (Include Area Code) (512) 536-3545	22c. OFFICE SYMBOL USAFSAM/VNBD

DD Form 1473, JUN 86 *Previous editions are obsolete.*

SECURITY CLASSIFICATION OF THIS PAGE

UNCLASSIFIED

19. ABSTRACT (Continued)

non-flowing conditions in oxygen tonometered blood. The next longest values for T_2 were in blood with fixed oxygen bubbles while the shortest was for blood with fixed nitrogen bubbles. From this data, it was concluded that it was feasible to use NMR measurements in blood to indicate the difference between fixed oxygen bubbles, fixed air bubbles, and fixed or flowing nitrogen bubbles in blood. When the bubbles were flowing, the values of T_2 were longer than when the bubbles were fixed. It was concluded that the values of T_2 for flowing bubbles may need to be corrected, with flow information from the NMR signal, to non-flow conditions for accurate indications of the onset of decompression bubbles. A follow-on program is recommended and a brief description of the tasks is given.

TABLE OF CONTENTS

LIST OF FIGURES

I. INTRODUCTION

A. Background

The probability that a decompressed subject will develop bends is thought to be related to the number of circulating bubbles. The quantity of bubbles is crudely estimated by a grading system developed by Newman, Hall and Lindaweaver[1]. Grade I represents a very few isolated bubble while grade IV, the maximum, represents continuously flowing bubbles. However the presence of intravascular bubbles (even grade IV) does not necessarily mean that bends will occur. An accurate prediction of bends would be useful in military and space operations as a warning device to crew members. In addition, laboratory research into bends would be less hazardous with an adequate prediction device.

In recent years, several investigators have considered methods to predict the onset of decompression sickness (DCS), sometimes called bends, by identifying the presence of "gas bubbles" in venous blood using the techniques of Doppler ultrasonics[2]. An Ultrasonic-Doppler Precordial Bubble Detector (UPBD), which is a modification of a Doppler Transcutaneous Blood Velocity Sensor, detects bubbles within the vascular system[2]. False alarms, particularly false positives, have caused concern regarding the value of the UPBD tool in determining the onset of DCS.[2]

The UPBD device has been found valuable in detecting the circulating bubbles that precede bends in hyperbaric decompressions. In subjects exposed to altitude decompressions, two problems have developed. The first is the one mentioned previously wherein false positives are occasionally found resulting from the presence of large numbers of bubbles in the blood which do not produce DCS. The second problem, of particular interest to altitude decompression is the lead time between the detection of bubbles to the development of DCS. It is important to warn of incipient bends soon enough before DCS develops.[2]

To better understand the onset and severity of DCS, additional information would be helpful. What is needed is to determine not only the concentration, in situ, in the joints but also where bubbles are formed. Are the bubbles formed in the joint capsule?; in the tendon sheath?; in the muscle bed?; or in other extravascular tissue? It is theorized that these bubbles form where the shear force is maximum in the fluid involved.[8,9]

B. Basic Measurement Method

Based upon the techniques and experience in magnetic resonance gained by SwRI personnel over the last 35 years, it was proposed that nuclear magnetic resonance be investigated as a means for providing answers to these questions and that the possibility of developing an NMR instrument be considered which can detect, in situ, the onset and concentration of bubbles.

A nuclear magnetic resonance (NMR) instrument give signal voltages which are proportional to the number of nuclei being resonated in a fixed magnetic field and to the effects of the surroundings of the nuclei being measured. When exposed to an appropriate radiofrequency electromagnetic field, the resonating nuclei absorb energy and are no longer in equilibrium with the surroundings. This energy is exponentially lost to the surroundings by two mechanisms; one between neighboring resonating nuclei and the second between the

resonating nuclei and the rest of the surroundings. The first, called the spin-spin relaxation mechanism, has a time constant labelled T_2. The second, called the spin-lattice relaxation mechanism, has a time constant labelled T_1. The values of T_1 and T_2 for liquids are directly proportional to the fluid viscosity, inversely proportional to the temperature and inversely proportional to the concentrations of paramagnetic ions such as Fe^{+++} and paramagnetic gases such as oxygen. Therefore, the values for the relaxation times T_1 and T_2 should be different for body fluids with oxygen, without oxygen, and with high concentrations of nitrogen.[10,11]

To allow the potential of NMR to be explored for this application, it was therefore proposed that a project be undertaken to determine the feasibility of using magnetic resonance techniques to measure the concentration of decompression bubbles through their effect on the relaxation times T_1 and T_2 of the hydrogen in the fluid or tissue in which they are contained. It was expected that favorable results from this feasibility investigation will provide the basis for further programs which will include the development of special magnetic resonance equipment for making measurements of the bubble concentration in the joints, tissue or blood of persons in pressure and altitude chambers. The proposal for the above feasibility project was submitted and accepted. The following sections give a summary of accomplishments, the objectives, the technical discussion, the experimental results, the basic equipment design concepts, the conclusions,and the recommendations.

II. SUMMARY OF ACCOMPLISHMENTS

The program was proposed in three tasks: (1) Modify the laboratory NMR equipment at SwRI and construct the bubble generator, (2) Make NMR measurements (T_1 and T_2) on blood samples both with and without bubbles of oxygen, air, and nitrogen, and (3) make a magnetic resonance image of a knee and determine the relaxation times (T_1 and T_2) in the synovial fluid.

The bubble generator in Figure 14 was constructed and tested successfully. The NMR detection head (RF detection coil and tuning capacitor) was modified to accept the bubble generator and useful NMR signals from blood were obtained. Blood samples were procured and NMR measurements were made on 26 samples, each prepared in a different way. For 18 of the samples, values of T_1 and T_2 were determined; for 7 of the samples, only T_2 values were derived; for one sample of oxygenated blood, only the value of T_1 was measured. In all of the samples, only one value of T_1 was obtained and the mean value for T_2 for all blood samples was 180 milliseconds with a standard deviation of 58 milliseconds and a range of 70 to 385 milliseconds. All of the blood samples had two values of T_2. The degassed plasma and the water samples had one value of T_2 and one value of T_1. The values of T_2 varied with percent oxyhemoglobin while T_1 did not. The value of T_2 is longest in oxygenated blood, slightly lower for blood with stationary oxygen bubbles, lower still for venous blood, and lowest for blood with nitrogen. The use of nitrogen bubbles causes the value of T_2 to be slightly higher than for blood tonometered with nitrogen. The values of T_2 are higher when the bubbles in the blood are flowing than when they are stationary. From these results, it is concluded that it is feasible that NMR measurements of T_2 in blood can be used to distinguish oxygenated blood from nitrated blood both without and with the gases in bubbles.

The magnetic resonance image (MRI) of the knee was made at a local hospital and the images were processed to obtain the values of T_1 and T_2 in the synovial fluid. Only one value of T_1 and one value of T_2 were measured. No source of synovial fluid was found outside of the body so that no NMR measurements were made with bubbles of gas in the synovial fluid. It is concluded from the MRI information that in-vivo NMR measurements can be readily made using a U-shaped magnet with an RF detection coil on the skin at a position so that the radiofrequency magnetic field of the RF detection coil has the desired values of frequency and intensity in the sac containing the synovial fluid. Thus it can be concluded that it is feasible to make in-vivo NMR measurements of the value of T_2 in the synovial fluids in the knee.

It is recommended that a 6-task follow-on program be undertaken to quantify the values of blood oxygenation and other blood characteristics so that graphs can be made of the NMR signal level as a function of percent oxygenation in blood, synovial fluid, and tissue. A brief description of these six tasks is included at the end of the report.

III. OBJECTIVES AND PROPOSED PROGRAM

A. Objective

The overall objective of the proposed program is to investigate experimentally the feasibility of the use of nuclear magnetic resonance for the detection of bubble formation in human joints using *in vitro* models to produce bubbles and examine the detection, quantification and sizing of bubbles.

B. Proposed Program

The proposed program is composed of three tasks a described in the following paragraphs.

1. Task A

The first task is to establish the means with which small bubbles of air can be generated in and removed from liquid samples located within the measurement region of an SwRI laboratory hydrogen transient NMR instrument. Once the means has been chosen, it will be implemented and the required RF detection coil will be designed and constructed. The NMR sensor (RF Coil and Magnet) will be connected to an existing SwRI laboratory NMR apparatus. The system will be configured to acquire and store the NMR data needed to calculate the values of T_1 and T_2 for each sample studied.

2. Task B

Using the NMR device modified and configured as in Task A, hydrogen transient NMR measurements will be made first on pure water from which the air and/or oxygen have been removed. The resulting data will be used to determine the values of the relaxation times T_1 and T_2 for this pure water. Bubbles of oxygen, natural air, artificial air and nitrogen will then be generated in the pure water. The hydrogen transient NMR measurements will be repeated and the relaxation times T_1 and T_2 calculated for the included-bubble conditions. Similar NMR measurements and T_1 and T_2 determinations will then be made (both with and without bubbles of oxygen and nitrogen using blood serum, synovial fluid, and whole blood.

3. Task C

Using the NMR Imaging device at Southwest Methodist Hospital, an NMR image will be made on one knee of one volunteer supplied by the sponsor. The position of the image slice will be chosen to display the maximum of the joint fluid. If possible at that state of the development of the work at the Methodist Hospital, values of T_1 and T_2, will also be determine at a selected point in the fluid.

4. Task D

The results from the above three tasks will be summarized in a final report and used in the proposal for the follow-on effort.

IV. TECHNICAL DISCUSSION

The effort proposed for this project is based upon the use of hydrogen transient NMR to sense the changes in the hydrogen NMR relaxation times (T_1 and T_2) of body fluids (blood and synovial) caused by the presence in these fluids of bubbles of paramagnetic gases such as oxygen or air and non-paramagnetic gases such as nitrogen. As will be shown later in this discussion, the presence of paramagnetic ions such as Fe^{+++} will drastically reduce the magnitude of T_1 and T_2 for the hydrogen nuclei in water. For dissolved oxygen in water, the values of T_1 and T_2 are reduced a lesser value. The evidence of relaxation time changes caused by gas bubbles has been studied much less than dissolved oxygen and paramagnetic ions and is the work proposed herein. Related topics briefly discussed in the following paragraphs, include (1) the phenomenon of NMR, (2) relaxation phenomena in NMR (3) the effects on NMR relaxation times of dissolved oxygen, nitrogen, and paramagnetic ions, (4) the NMR instrumentation experience at SwRI which can be used for development, when feasibility is assured, of instrumentation to make bubble concentration measurements in the blood and joints of persons in pressure and/or altitude chambers, and (5) the work already accomplished in detecting bubbles in blood.

A. The NMR Phenomena

Nuclear Magnetic Resonance (NMR) involves the resonant absorption by nuclei located in a pair of quadrature magnetic fields[1,2]: one fixed field, H_0, and the other a radiofrequency (RF) field, $2H_1 \text{Cos} 2\pi f t$. The fixed field H_0 cause the nuclei to be in the state to absorb energy from the RF magnetic field and permit qualitative and quantitative analysis when the RF frequency, f_0, is made equal to the product of the constant γ (for the selected nucleus) multiplied times the strength of the fixed magnetic field, H_0. The constant, γ, for hydrogen nuclei is 4258 Hertz per Gauss. Qualitative analysis comes by choosing the ratio H_0/f_0 for the particular nuclei desired to be resonated.[1,2]

The rate at which energy is absorbed by the nuclei is directly proportional to the number of absorbing nuclei contained within the volume of material sampled by the RF detection coil used to produce the RF field, H_1. This gives quantitative analysis.[1,2] Thus, NMR gives a voltage proportional to the number of resonating nuclei in the sampled volume of material.

When nuclei absorb energy, the equilibrium between the nuclei and their surroundings is changed which causes the absorbed energy to be exchanged exponentially with the surroundings by two mechanisms[3,4]. One with a time constant of T_2 involves the exchange between neighboring resonating nuclei i.e., nuclei of the same isotope. The second with a time constant T_1 is for the exchange between resonating nuclei and the rest of their surroundings. The time constant T_2 is called the spin-spin relaxation time, while the time constant T_1 is called the spin-lattice relaxation time. A more complete discussion of the NMR phenomenon is given in references (1) and (2).

B. NMR Effects of Viscosity

For a first approximation of T_1 and T_2, it is assumed that everything in the material is fixed and that the relative position coordinates describing the location are constants for the nuclei and the lattice. In reality, however, the position coordinates themselves are functions of time. In liquids, the Brownian motion is described by a

correlation time τ_c, which is the time that it takes a molecule in an electric field to rotate over such an angle that the relative positions of the nuclei with respect to the external field have changed appreciably. In the calculation of this change, the rotation is separated from the translation. Thus, the spin-lattice relaxation time, T_1, is calculated from two separate calculation $(1/T_1)_{rot.}$ which is the part due to rotation, and $(1/T_1)_{trans.}$, which is the translation part. The spin-lattice relaxation time comes from[4]

$$\frac{1}{T_1} = \frac{1}{(T_1)_{rot.}} + \frac{1}{(T_1)_{trans.}} \tag{3}$$

For water, Bloembergen[7] has calculated the rotational component to be

$$\frac{1}{(T_1)_{rot.}} = 0.9G^4\gamma^2b^{-6}\tau_c \tag{4}$$

where γ is the gyromagnetic ratio for the nuclei involved, b is the distance between neighboring nuclei of the same isotope, and τ_c is the correlation time as described above. It was further shown that

$$\tau_c = \frac{4}{3}\pi\eta a^3/kT \tag{5}$$

where η is the viscosity of the liquid, a is the diameter of the molecule containing the nuclei, k is Boltzmann's constant, h is Plank's constant, and T is the temperature on the absolute (Kelvin) scale. Therefore, because the correlation time is directly proportional to the viscosity, the value of $(T_1)_{rot.}$ is then inversely proportional to viscosity in liquids. For water, Bloembergen[7] also calculated that the translational component is

$$\frac{1}{(T_1)_{trans.}} = 0.9\pi^2\gamma^4h^2\eta N/2\pi kT. \tag{6}$$

Again, the value of $(T_1)_{trans.}$ varies inversely with the viscosity.

As a test of the above inverse dependence of T_1 on viscosity, Bloembergen[7] measured the value of T_1 for hydrocarbon liquids having viscosity ranging from 0.48 to 260 centipoise. In the graph of the resultant data, Figure 1, the inverse dependence of T_1 upon viscosity is readily observed.

The theory developed by Bloembergen[4] and Casper[5] showed that when the motions were the vibrations of solids, then the value of T_1 varied directly as the value of the correlation time τ_c. Some measurements were made on ice as the correlation time was altered by varying the temperature. The results are shown in graphical form in Figure 2. The direct variation of T_1 with the (Debye) correlation time τ_c is very evident in Figure 2.

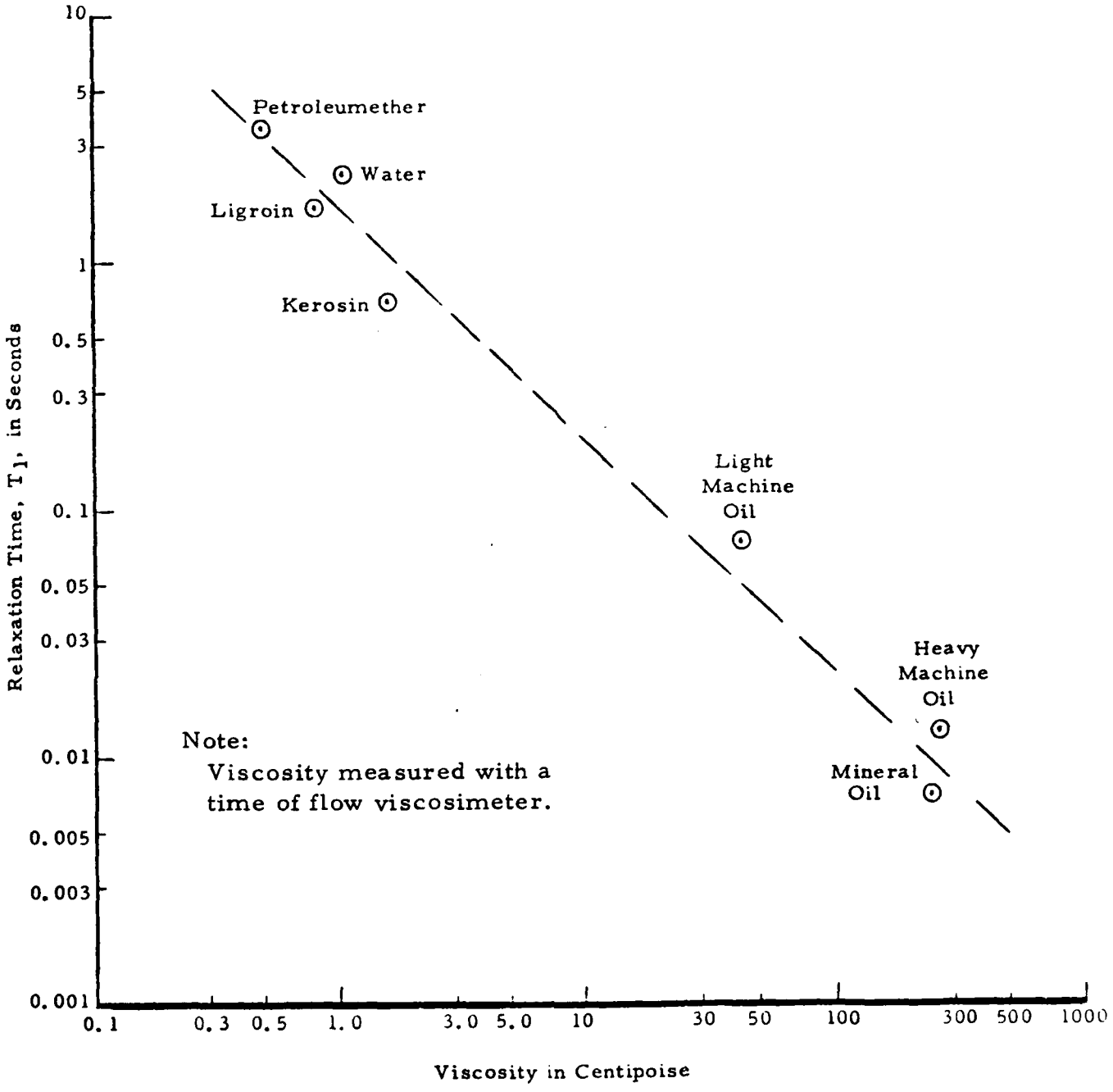

FIGURE 1 GRAPH OF THE SPIN-LATTICE RELAXATION TIME AS A FUNCTION OF VISCOSITY FOR SEVERAL MATERIALS.

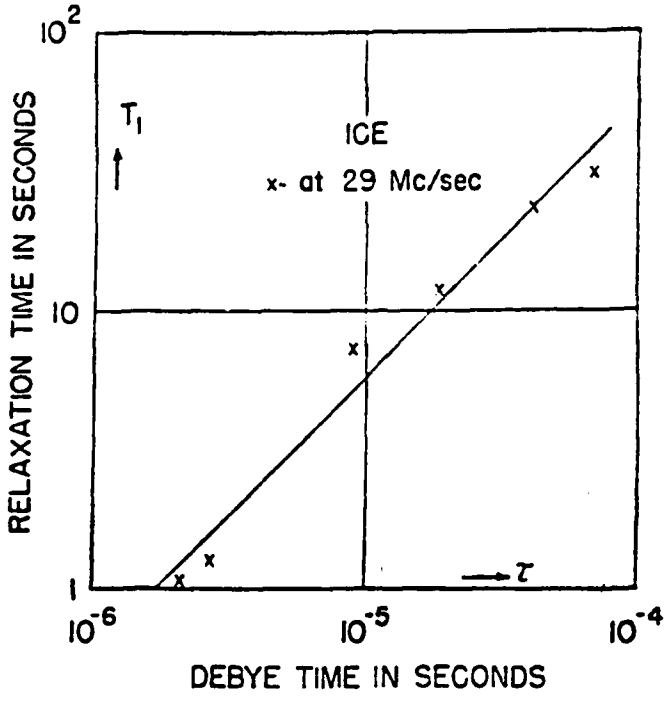

FIGURE 2 THE RELAXATION TIME OF THE PROTON RESONANCE IN ICE BETWEEN -2°C AND -40°C, PLOTTED AGAINST THE DEBYE TIME τ. The line drawn through the experimental points, makes an angle of 45° with the positive X-axis. (1)

Bloembergen has drawn a graph, reproduced as Figure 3, which represents how T_1 and T_2 vary with the correlation time τ_c. Below a certain value of τ_c, both T_1 and T_2 are inversely proportional to τ_c and thus to viscosity since τ_c and viscosity are directly related. Above this critical point, T_1 becomes directly dependent upon τ_c while T_2 remains inversely dependent until T_1 reaches an asymptotic value. Thus, it appears from Figures 1, 2, and 3, that the value of the viscosity of liquids, plastics, and solids could be determined from measurements of both T_1 and T_2.

The above description of relaxation time considered only pure materials. When different liquids are mixed or when liquids are absorbed or adsorbed by solids, then a different description of relaxation time must be considered. The Zimmerman Brittin model[8] for impure materials is a stochastic one which states, in its most general form, that the absorbing nuclei can be considered as a spin system composed of a finite number of phases with each phase characterized by a single relaxation time. There is an exchange of spins among the various phases which can be described by means of a stationary Markoff process. This leads to a very complex result which does not lend itself to analytical solution. However, there igure 1 are two asymptotic expressions which can give analytical solutions. These are for the conditions, (a) where there is a very slow exchange relative to the relaxation times involved, and (b) where there is a very rapid exchange relative to the relaxation times involved.

For the rapid exchange condition, there will be one value of either T_1 or T_2 which is a composite of the separate decay rates for the components comprising the material. For example, if there are two components each with a different relaxation decay rate (T_{21} and T_{22} for example), then the transient NMR signal voltage decays at a single-exponential rate (T_2) which is given by

$$v_f = V_o \exp \frac{-t}{T_2}, \text{ where } \frac{1}{T_2} = \frac{P_1}{T_{21}} + \frac{P_2}{T_{22}} \tag{7}$$

In Equation (7), P_1 is the fraction of the absorbing nuclei in the first phase with a relaxation time value of T_{21}; P_2 is the fraction in the second phase with T_{22}, and V_o is the value of v_f at t = o. The concentrations of the two components can be determined from the NMR measurements if the values of T_{21} and T_{22} are known for each component separately since $P_1 + P_2 = 1$.

For the slow-exchange situation, two or more widely-separated values of relaxation time can exist, one for each component. The NMR signal voltage for a two-component, slow-exchange condition is,

$$v_s = V_1 \exp. \frac{-t}{T_{21}} + V_2 \exp. \frac{-t}{T_{22}} \tag{8}$$

where T_{21} and T_{22} are the spin-spin relaxation times for the two constituents and V_1 and V_2 are proportional to the concentrations of these constituents in the sample at t = 0. In many materials, such as water in plants, the values of T_{21} and T_{22} are sufficiently different for the two constituents so that NMR measurements provide an accurate quantitative measure of the

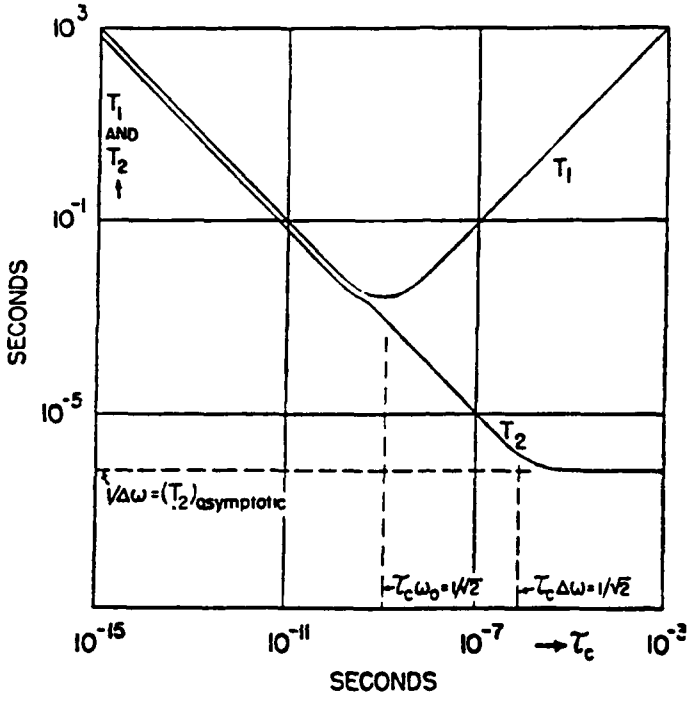

FIGURE 3 THE THEORETICAL BEHAVIOUR OF THE RELAXATION TIME T_1 AND T_2 WHICH IS A MEASURE FOR THE INVERSE LINE WIDTH.[1]

concentrations of each component.

Experience at SwRI over the last 35 years has shown that water in plants and seeds is usually held in two or more discrete binding states. There is a rapid exchange between the hydrogen in the water of each binding level of water on substrate. Each rapid exchange system gives a different value of T_2 from equation (7). Thus, there will be two values of T_2 for water in two binding phases, T_{21} and T_{22}. If there is hydrogen also in the substrate, it will have a relaxation time, T_{23}, different from those of the water binding phases. Therefore, the NMR signal for this three-phase condition will be

$$v = V_1 \exp\frac{-t}{T_{21}} + V_2 \exp\frac{-t}{T_{22}} + V_3 \exp\frac{-t}{T_{23}} \qquad (9)$$

When these values are sufficiently different one from the other, then the concentrations of each water phase can be obtained from

$$\text{Percent Water in First Phase} = \frac{k_1 V_1}{V_1 + V_2 + V_3} \qquad (10)$$

$$\text{Percent Water in Second Phase} = \frac{k_2 V_2}{V_1 + V_2 + V_3} \qquad (11)$$

The percentage of total water can be obtained by adding Equations (10) and (11). The constants k_1 and k_2 are needed to convert the voltage ratios to weight percent water.

When the two parts of some epoxies are first mixed the NMR signal will show two distinct relaxation times. After a short period when the two parts start to mix or chemically interact, the two values will change to one value. This one value of the relaxation time, T_2, will decrease as the epoxy cures, arriving at a relatively low value when the epoxy is fully cured. The value of T_2 for the two components will first decrease in value and then increase in value according to Figure 3. The values of T_1 and T_2 can therefore describe the state of the cure.

C. The Effects of Paramagnetic Ions and Gases

For pure water at room temperature[4], the relaxation times T_1 and T_2 are essentially equal to 2.8 seconds due solely to the interaction between the hydrogen nuclei. When a paramagnetic solute is added to water, the relaxation times T_1 and T_2 are considerably shortened. The presence of paramagnetic ions such as Fe^{+++} in the water from the paramagnetic solute increases the coupling between the resonating nuclei (hydrogen nuclei in water) and thus reduces the relaxation times. The equation for $1/T_1$ is then[4]

$$\frac{1}{T_1} = 0.9\pi_p^2 h^2 \mu_{eff}^2 N_{ion} \eta / 5kT \qquad (12)$$

where μ_{eff} is the magnetic moment for the paramagnetic ion, N_{ion} is the number of ions per cm^3 and γ is the magnetic moment for the hydrogen nucleus, a proton. The value of μ_{eff} is about a million times larger than γ and a small concentration of paramagnetic ions causes the relaxation times to be considerably shortened. For example, 10^{-3} moles per liter of Mn++ ions in water reduces T_2 from 3.6 seconds to 0.1 seconds.

The influence of oxygen gas dissolved in water is less than that of dissolved paramagnetic ions because the oxygen is not highly soluble in water. The maximum concentration of dissolved Oxygen in water at room temperature and a pressure of 0.18 atmospheres is around 1.5×10^{17} molecules/cm^3. This concentration of the paramagnetic gas Oxygen reduces the relaxation time for water from 2.8 to 2.5 seconds[4].

Measurements have also been made on the effect of dissolved oxygen concentration on the relaxation times of not only water but also ethyl alcohol and benzene[6]. The graph of $1/T_1$ as a function of the concentration of dissolved oxygen molecules in water, ethyl alcohol and benzene is given in Figure 4.

With the brief library search undertaken to write the proposal, one reference[7] was found in which NMR relaxation times were measured in whole blood and blood plasma. The authors oxygenated the samples by bubbling moist air through the sample for at least 20 minutes. The samples were deoxygenated by bubbling nitrogen. the values of relaxation time T_1 obtained for venous blood (deoxygenated) is 0.599 seconds at an NMR frequency of 6 MHz (1410 Gauss). Oxygenated blood had a T_1 value of 0.559 seconds. The deoxygenated plasma had a T_1 value of 1.171 seconds while the oxygenated plasma had a T_1 value of 1.098 seconds. Some blood from a blood bank gave a T_1 of 0.744 seconds.

D. NMR Instrumentation

The manner in which the nuclear magnetic resonance signal is usually obtained is shown in Figure 5, where the steady magnetic field of strength H_o is supplied by the magnet and the RF magnetic field, of strength H_1 and frequency f_o, is supplied by the radiofrequency coil. When the ratio of f_o/H_o is set to the hydrogen value of 4.258 MHz per Gauss, and when the direction of H_1 is perpendicular to H_o, as shown in Figure 5, then a transient hydrogen NMR signal can be obtained from all of the hydrogen nuclei in the effective volume of the radiofrequency coil.

These same resonance conditions, however, can be obtained outside of the magnet and outside of the RF coil as shown in Figure 6. In the sensitive region the ratio of f_o/H_o and the perpendicular field conditions are satisfied so that NMR signals can be obtained from hydrogen nuclei in the sensitive volume. As the strength of the magnetic field, H_o, is increased, the position of the sensitive volume will move further away from the magnet; as the field is decreased, the sensitive volume moves closer. With this method the hydrogen transient NMR signal can be obtained from a selected sensitive volume of material lying outside the detection probe. The sensitive region in Figure 6 can be scanned through the thickness of the material by proper choice of the field intensity. This type of detection head can be mounted below a moving belt as shown in Figure 7 to measure the concentration of the resonated nuclei in the material carried on the belt and the position of the sensitive volume can be adjusted by changing the strength of the magnetic field.

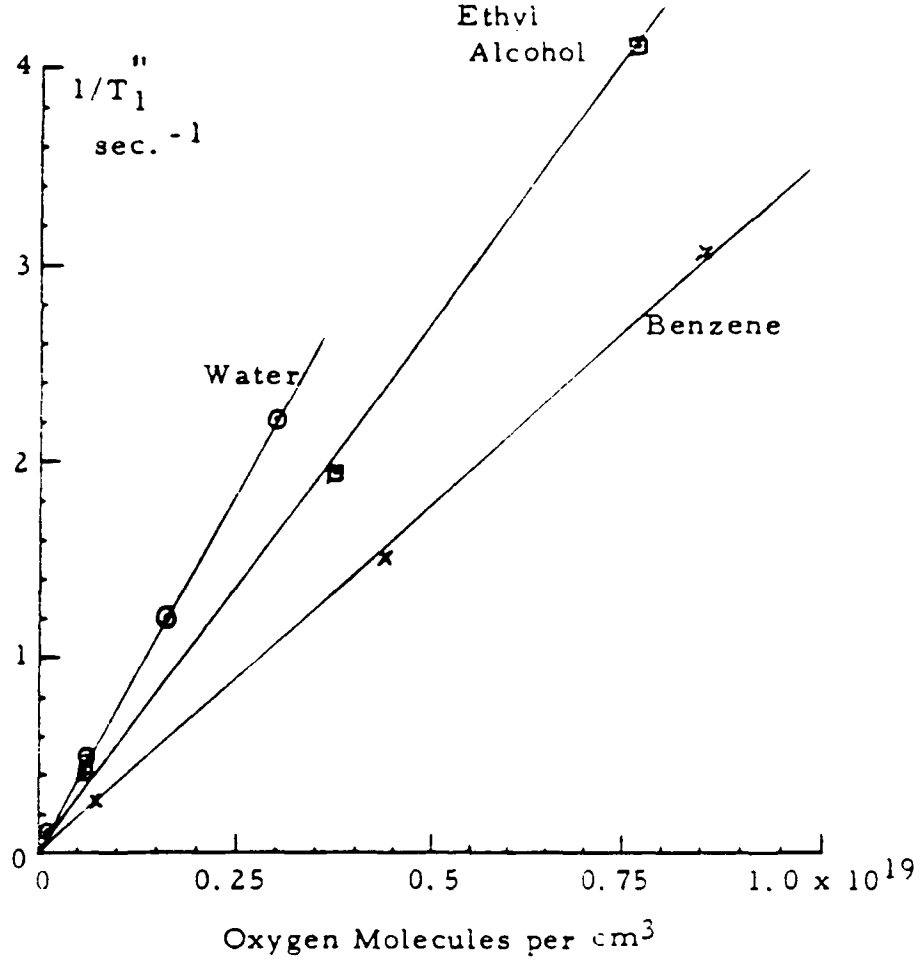

4940

FIGURE 4. GRAPH OF $1/T_1''$ AS A FUNCTION OF THE NUMBER OF DISSOLVED OXYGEN MOLECULES PER CM^3 FOR THREE LIQUIDS AT A TEMPERATURE OF 20°C. THE MEASUREMENTS WERE MADE AT 7MHz.[6]

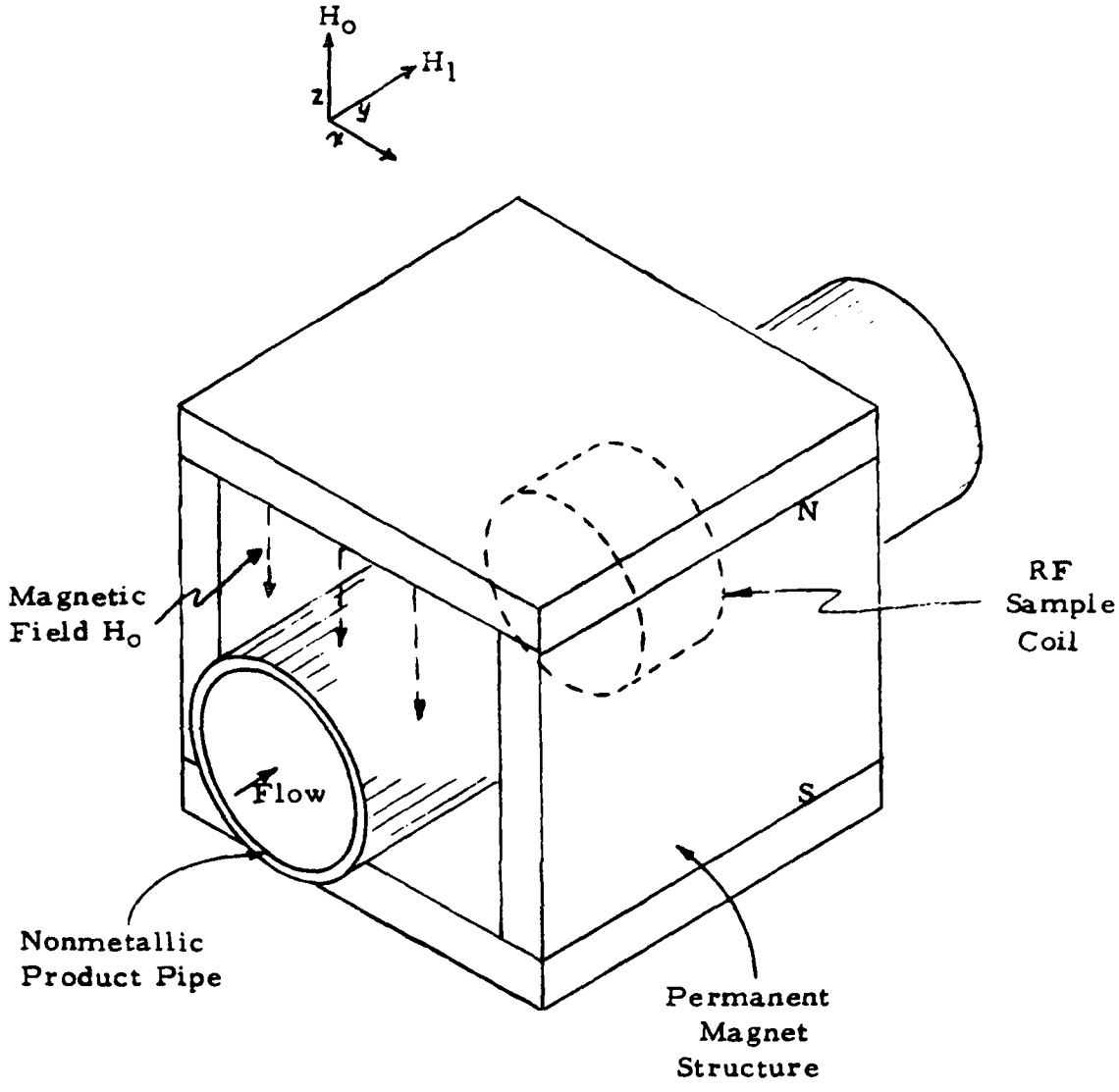

4988b

FIGURE 5 . SKETCH ILLUSTRATING THE SENSING HEAD CONCEPT FOR THE MAGNETIC RESONANCE COMPOSITION B INSTRUMENTATION

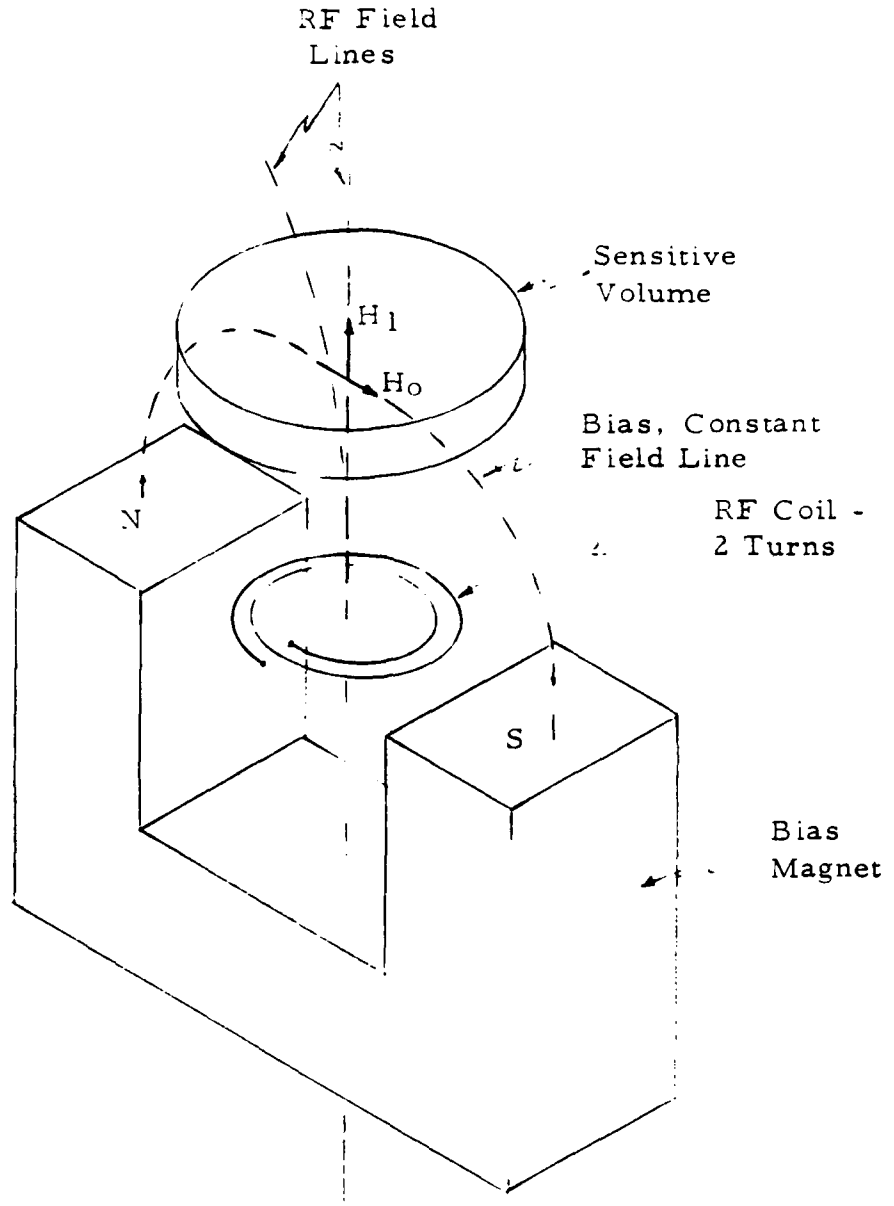

2464

FIGURE 6. SCHEMATIC DIAGRAM OF A NMR DETECTION HEAD WHERE THE SENSITIVE VOLUME IS OUTSIDE OF THE MAGNET AND RF COIL CONFIGURATION

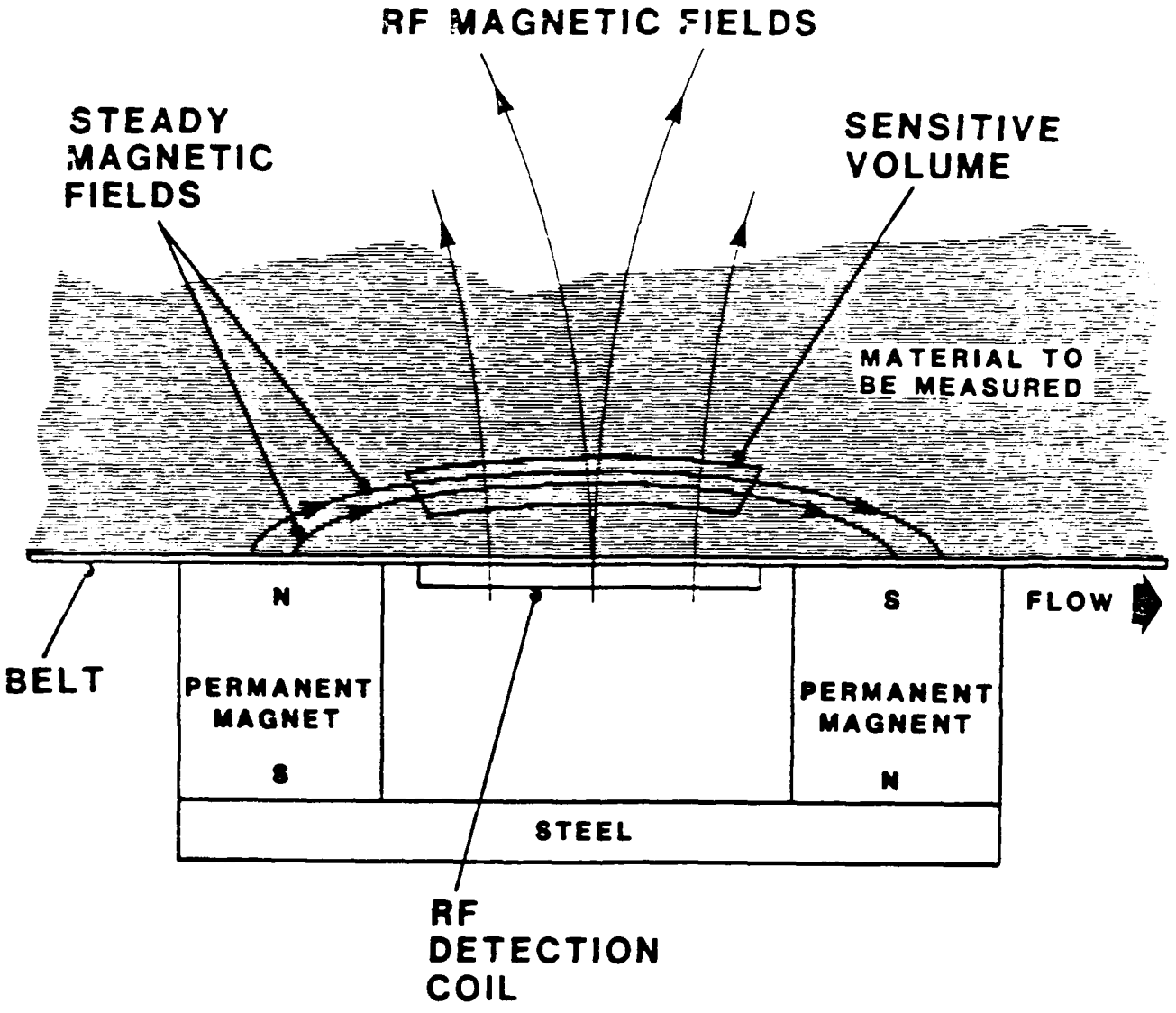

FIGURE 7 - CONFIGURATION OF AN NMR DETECTION HEAD COMPOSED OF A MAGNET AND AN RF DETECTION COIL FOR MOISTURE MEASUREMENTS IN MATERIAL FLOWING ON A BELT

The thickness and the shape of the sensitive region is controlled by the magnet inhomogeneity, the shape of the magnetic field, and the width of the NMR absorption curve. Sensitive volume thicknesses in the range of 1/16" to 1/4" can be readily obtained from an NMR detection head of the type shown in Figure 6.

Greater sensitivity can be achieved when the sample fills the magnet volume, as shown in Figure 5. The largest magnet-RF coil sampling volume developed to date at SwRI is one that is 14" high, 24" wide and 30" deep, but this is not a limit. Such a magnet and RF coil system, for example, can make NMR measurements in materials in 100 lb. sacks, on 24" wide V-belts and in pipes up to 14" O.D. The water concentration can be determined in appropriate materials which are contained in or carried by non-conductive and non-metallic conveyor belts or in pipes. Where NMR is to be applied to materials carried in metallic pipes, it is necessary to insert a non-conductive and non-metallic section at the NMR detection head shown in Figure 6.

Small detection heads can be designed to be buried in the material to be measured. For example, a 3" x 2" x 2" magnet-coil configuration like that in Figure 5 has been used to permanently monitor soil moisture under highway pavement. It could be buried in piles of materials to measure the concentration of specific nuclei, that is, water in grain by using hydrogen nuclei.

A block diagram of the electronic system generally associated with an NMR instrument is shown in Figure 8. Signals from the computer control the Magnet Current Programmer, the Digitizers and Memories in channels 1 and 2, the RF switch and the pulse programmer. The pulse sequences chosen by the computer controls operation of the RF switch and the two digitizers. The RF switch controls operation of the transmitter, receiver, and quadrature detector. The RF pulses from the transmitter are fed through the transmit side of the TR network to the RF detection coil in the magnetic field. The NMR signal comes from the RF detection coil through the receiver side of the TR network to the receiver where it is amplified and detected in the quadrature detector. The quadrature detector output has two components: in-phase and quadrature-phase. The in-phase component goes to the digitizer and memory in channel 1 and the quadrature-phase component goes to the digitizer and memory in channel 2. When the computer reaches the computation part of the program, it calculates the NMR signals as the square root of the sum of the squares of the channel 1 and channel 2 components and stores the resulting NMR signal in memory.

The system in Figure 8 is based on the use of a personal type computer, like the IBM PC, for control of the data acquisition, the signal processing and the signal storage. The block diagram of the computer interface is also shown in Figure 8. When instructed to start, through the keyboard or from an external start pulse, the computer program controls the NMR equipment through the selected sequences, receives the acquired data and stores it. The stored data can be used for further calculation as desired.

The electronics for NMR instrumentation is packaged in a way suitable to the application. One typical package, shown in Figure 9, is an NMR moisture meter for composite materials (plastic laminate samples) developed for the Army Materials and Mechanics Research Center[9]. In the photo, the upper part of the instrument contains the pulse programmer, the RF switch, the digitizers and memories for channels 1 and 2, and the magnet current programmer. The middle chassis contains the transmitter, the receiver and RF gate, the TR network and the

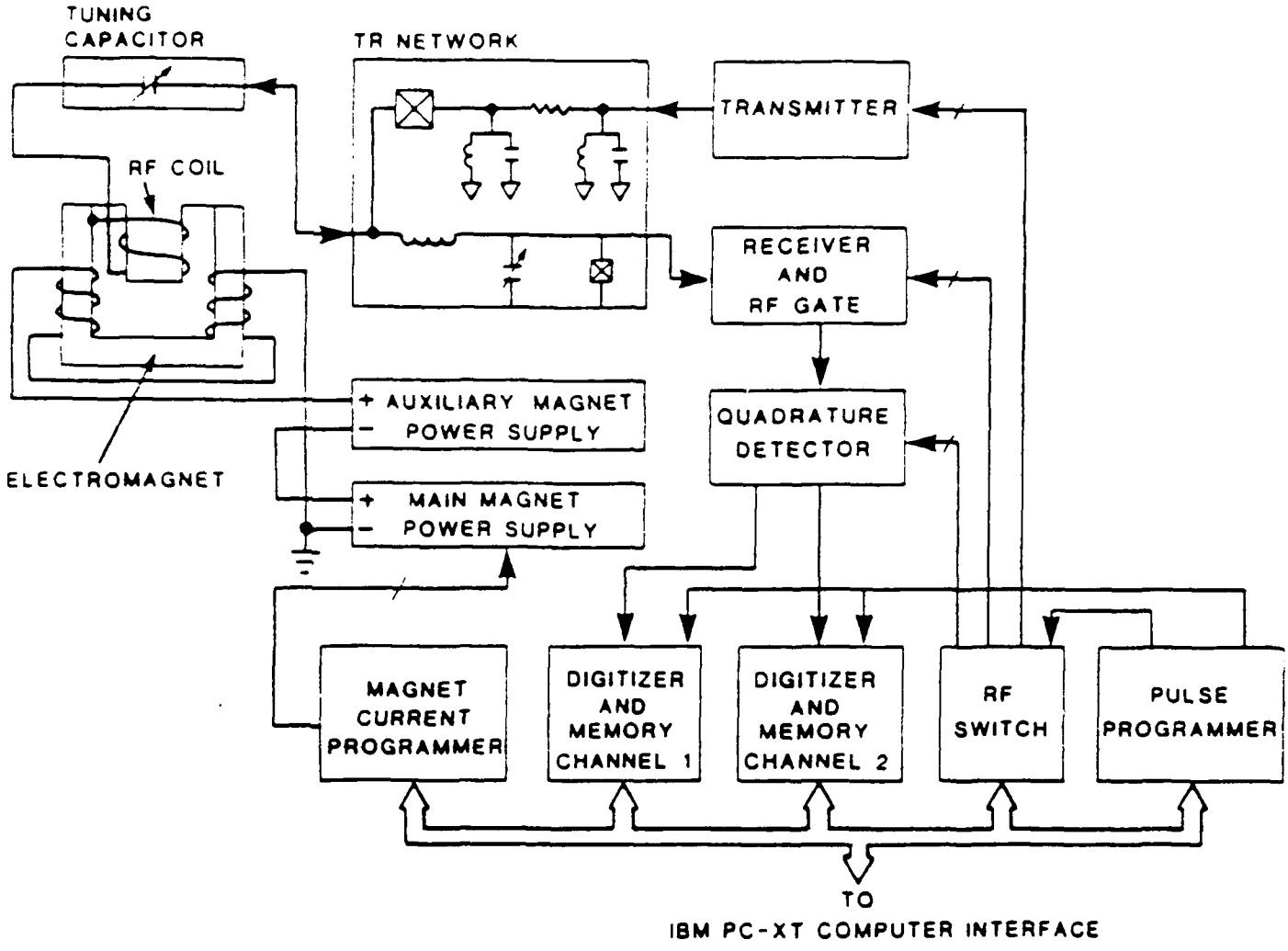

FIGURE 8 - BLOCK DIAGRAM OF THE COMPONENTS OF A COMPUTER CONTROLLED NUCLEAR MAGNETIC RESONANCE DEVICE CAPABLE OF DETERMINING THE WATER AND CONCENTRATION IN MATERIALS

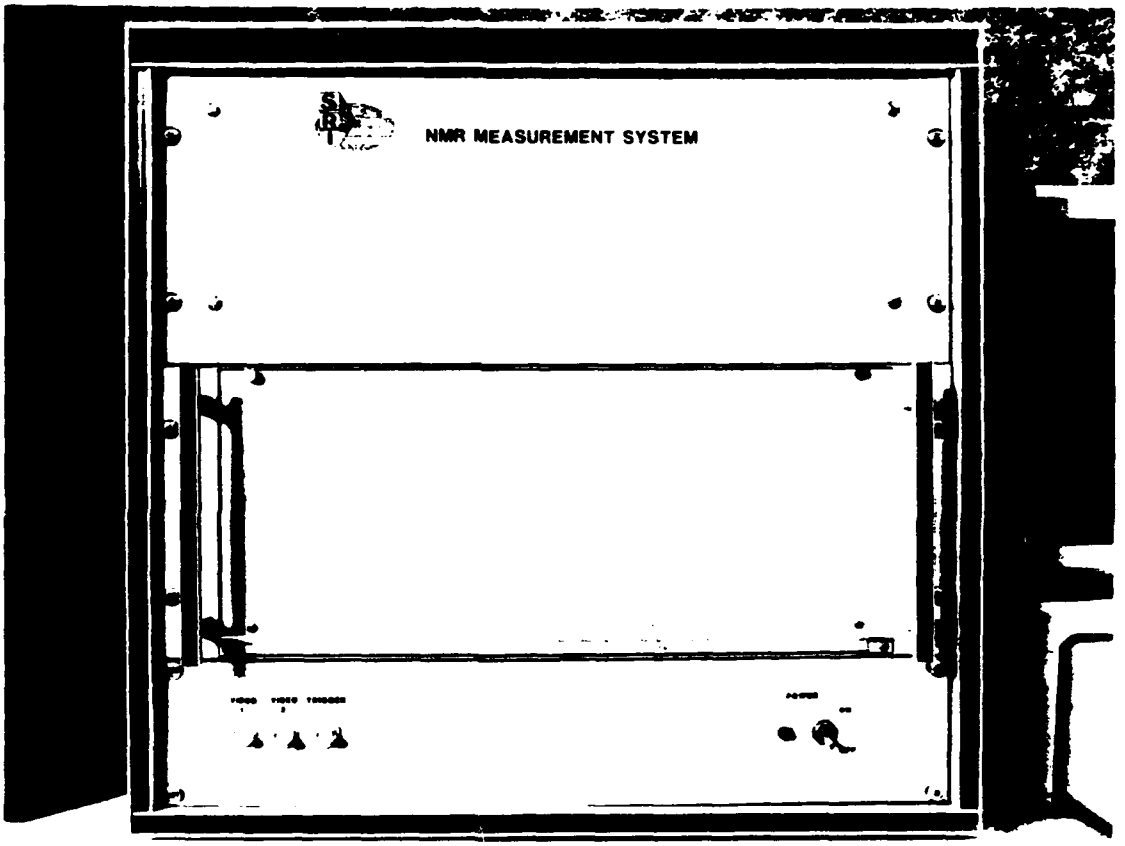

Figure 9. Example of the Electronics Package Which May Be Used for the NMR Device to Measure the Concentration of Water and Menthol in Tobacco.

quadrature detector. The bottom chassis contains the power supplies and the output connections to an oscilloscope. Since the electronics in Figure 9 is for an NMR device which uses a permanent magnet, no magnet power supply is needed.

E. Previous Measurements of Bubbles of Blood

The probability that a decompressed subject will develop bends is thought to be related to the number of circulating bubbles. The quantity of bubbles is crudely estimated by a grading system developed by Neuman, Hall, and Lindaweaver[8]. Grade I represents a very few isolated bubbles while grade IV, the maximum, represents continuously flowing bubbles. However, the presence of intravascular bubbles (even grade IV) does not necessarily mean that bends will occur[9]. An accurate prediction of bends would be useful in military and space operations as a warning device to crew members. In addition, laboratory research into bends would be less hazardous with an adequate prediction device.

In recent years, several investigators have considered methods to predict the onset of decompression sickness (DCS), sometimes called bends, by identifying the presence of "gas bubbles" in venous blood using the techniques of Doppler ultrasonics[9]. An Ultrasonic-Doppler Precordial Bubble Detector (UPBD), which is a modification of a Doppler Transcutaneous Blood Velocity Sensor, detects bubbles within the vascular system[9]. False alarms, particularly false positives, have caused concern regarding the value of the UPBD tool in determining the onset of DCS[9].

The UPBD uses a transducer which consists of two piezoelectric crystals mounted in plastic such that when electronically excited, the ultrasonic beams cross at a distance of 5 cm in front of the transducer. One crystal is driven by the transmitter and the other gives a voltage, proportional to the received ultrasonic signal, to the receiver. For bubble detection, the transducer is placed on the chest along the sternum at the third or fourth intercostal space on the left. The ultrasound waves from the transmitter-fed crystal pass into the chest where they strike the blood column in the pulmonary orthoprecordium of the heart and are reflected into the receiver crystal. The signal voltage from the receiver crystal is amplified by the receiver and compared in frequency with the voltage fed to the transmitter crystal. Any frequency difference is proportional to the Doppler frequency which is in turn proportional to the velocity of the blood in the pulmonary artery. The presence of bubbles is detected by the distinctive sound they produce in the flow signal[9].

The UPBD device has been found valuable in detecting the circulating bubbles that precede bends in hyperbaric decompressions. In subjects exposed to altitude decompressions, two problems have developed. The first is the one mentioned previously wherein false positives are occasionally found resulting from the presence of large numbers of bubbles in the blood which do not produce DCS. The second problem, of particular interest to altitude decompression is the lead time between the detection of bubbles to the development of DCS. It is important to warn of incipient bends soon enough before DCS development[9].

F. Blood Oxygenation Measurements in the Literature

The first part of the program was a literature search on nuclear magnetic resonance (NMR) measurements in blood. Two papers[10, 11] were found on the determination of T_2 (the spin-spin relaxation time) in the water in blood. It was found that T_2 is linearly

related over a large range to the blood oxygenation in percent oxyhemoglobin as shown in Figure 10. It was further stated that the value of T_1 (spin-lattice relaxation time) is independent of oxygenation.[10] A change in the composition of inhaled gases from 50% oxygen to 10% oxygen in normal blood without nitrogen reduced the value of T_1 for arterial blood by half or from 165 milliseconds to 80 milliseconds, corresponding to a decrease in blood oxygen content of about 45%. The high value of T_1 and hence the high blood oxygenation was restored in a short time by reverting from the 10% to the 50% oxygen inhaled gas. It has not yet been determined what effect a small concentration of oxygen has in the presence of a high concentration of nitrogen.

The second paper also describes a hydrogen NMR technique by which the blood oxygenation in percent oxyhemoglobin can be determined. The inhaled gas composition was changed to vary the percent oxyhemoglobin so that changes in T_2 can be determined. The inhaled gas composition was changed to vary the percent oxyhemoglobin from 10 to 99 percent which caused the value of T_2 to vary from 20 milliseconds to 140 milliseconds. When the inhaled gas was changed from a very low to a high percentage oxygen, the percent oxyhemoglobin reached a maximum in about 250 milliseconds.

The above two references have shown that the blood oxygenation in percent oxyhemoglobin can be measured in vitro with nuclear magnetic resonance techniques. They do not, however, indicate the NMR instrumentation which could be used to perform these measurements in vivo. The nearly 35 years experience at SwRI in the development of specialized NMR instruments has led us to the belief that at least three devices using NMR techniques can be used to determine, in vivo, in arterial or venous blood, the value of the T_2 for the hydrogen in the water in the blood. When the value of T_2 is entered into a calibration curve similar to Figure 10, the percent oxyhemoglobin can be obtained. Three different configurations of NMR instrumentation can be envisioned for determining the blood oxyhemoglobin.

The first manifestation is in Figure 11. The blood vessel in which the NMR measurements are to be made is inserted into a large magnetic field. As shown in Figure 11, an artery or a vein can be measured when the arm is shown inserted into the magnetic field. The RF detection coil should be placed perpendicular to the steady magnetic field from the magnet to obtain the greatest sensitivity. With this arrangement, the spin-spin relaxation time (T_2) of the water in the blood can be determined from the NMR data and converted into percent oxyhemoglobin using a calibration curve similar to Figure 10.

The second manifestation is sketched in Figure 12. Here, a portable NMR detection head (magnet plus RF detection coil) is placed over a blood vessel in the arm or other place on the person. The magnetic field of the U-shaped magnet in the blood vessel should be horizontal and the radiofrequency magnetic field from the RF detection coil should be vertical in the blood vessel to obtain the best sensitivity. With the configuration in Figure 12, the value of T_2 (spin-spin relaxation time) for the water in the blood in the vein or artery can be measured. Again, this value of T_2 can be converted into percent oxyhemoglobin using a calibration curve similar to Figure 10.

The third configuration is sketched in Figure 13. The two short, cylindrical magnets are placed opposite each other on opposite sides of an earlobe or a finger. The direction of the steady magnetic field is from one cylindrical magnet to the opposite

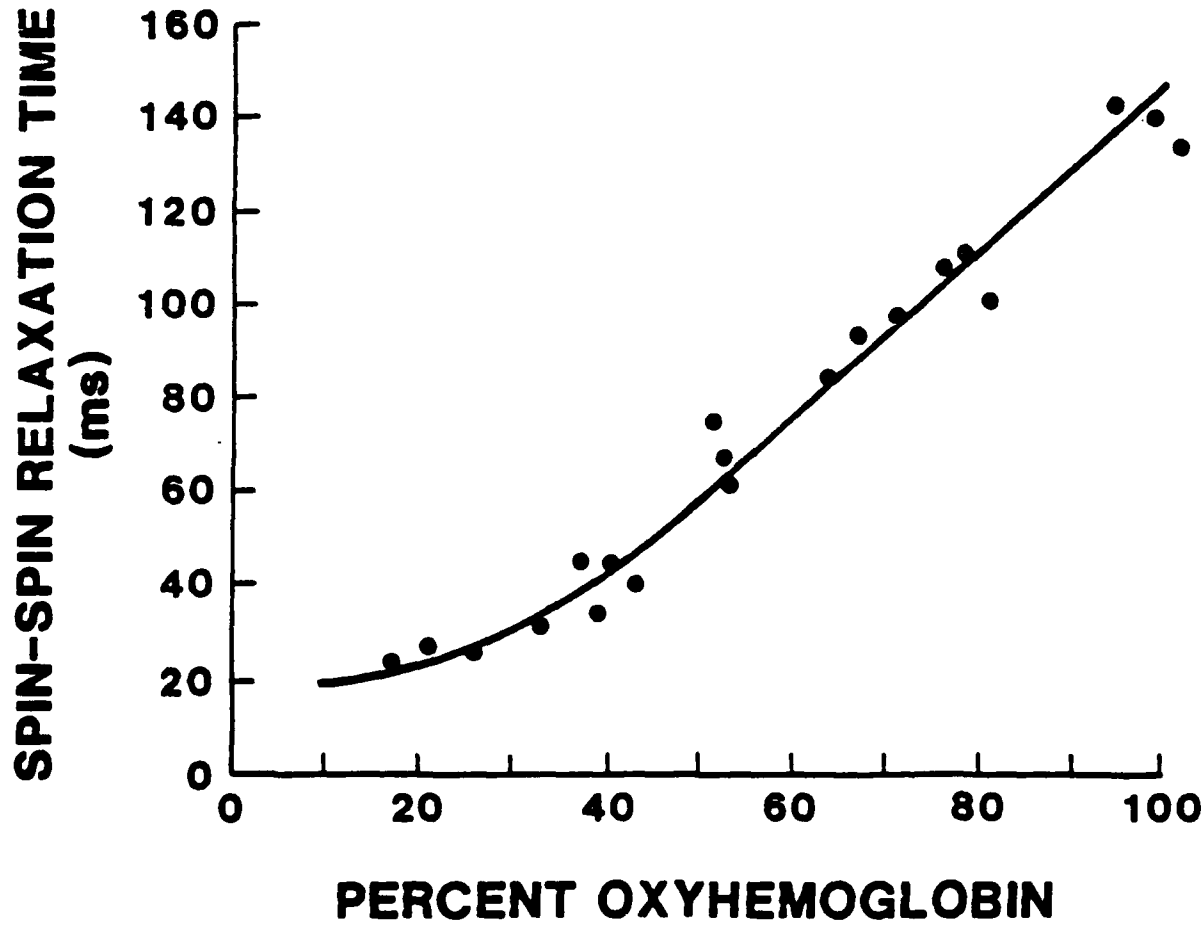

7692

FIGURE 10. BLOOD OXYGENATION IN PERCENT OXYHEMOGLOBIN AS A FUNCTION OF BLOOD WATER HYDROGEN SPIN-SPIN RELAXATION TIME (T_2) IN MILLISECONDS[12].

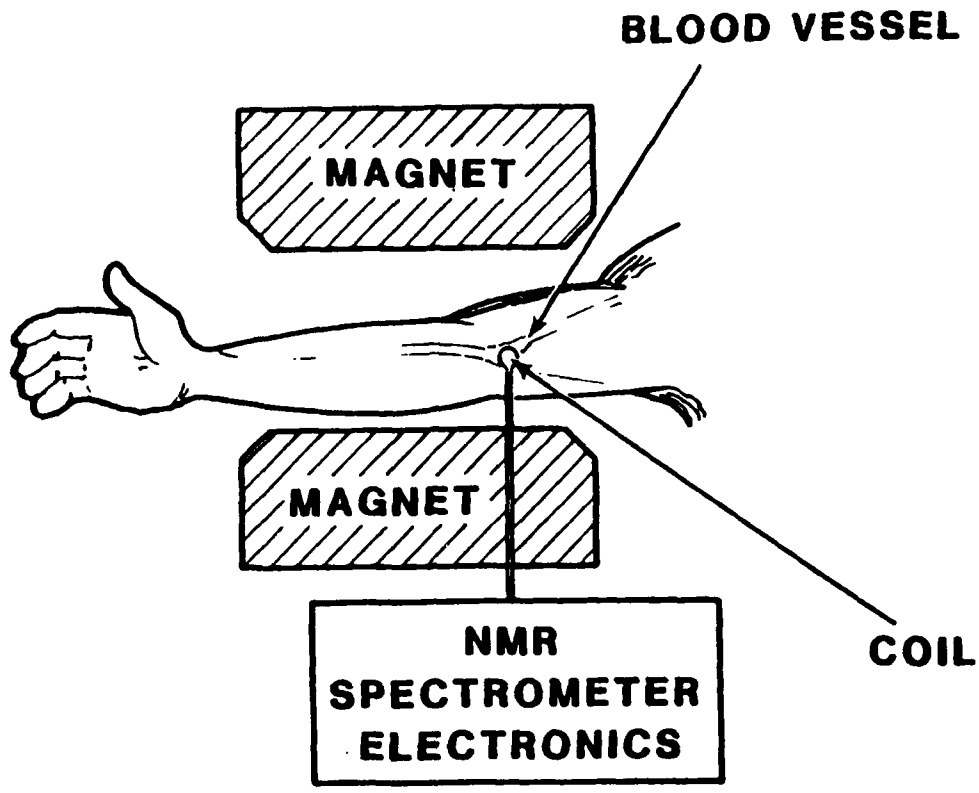

7693

FIGURE 11. BLOCK DIAGRAM OF THE DETECTION COIL, THE MAGNET AND THE NMR SPECTROMETER ELECTRONICS USED TO DETERMINE THE PERCENT OXYHEMOGLOBIN IN THE BLOOD IN THE BLOOD VESSEL.

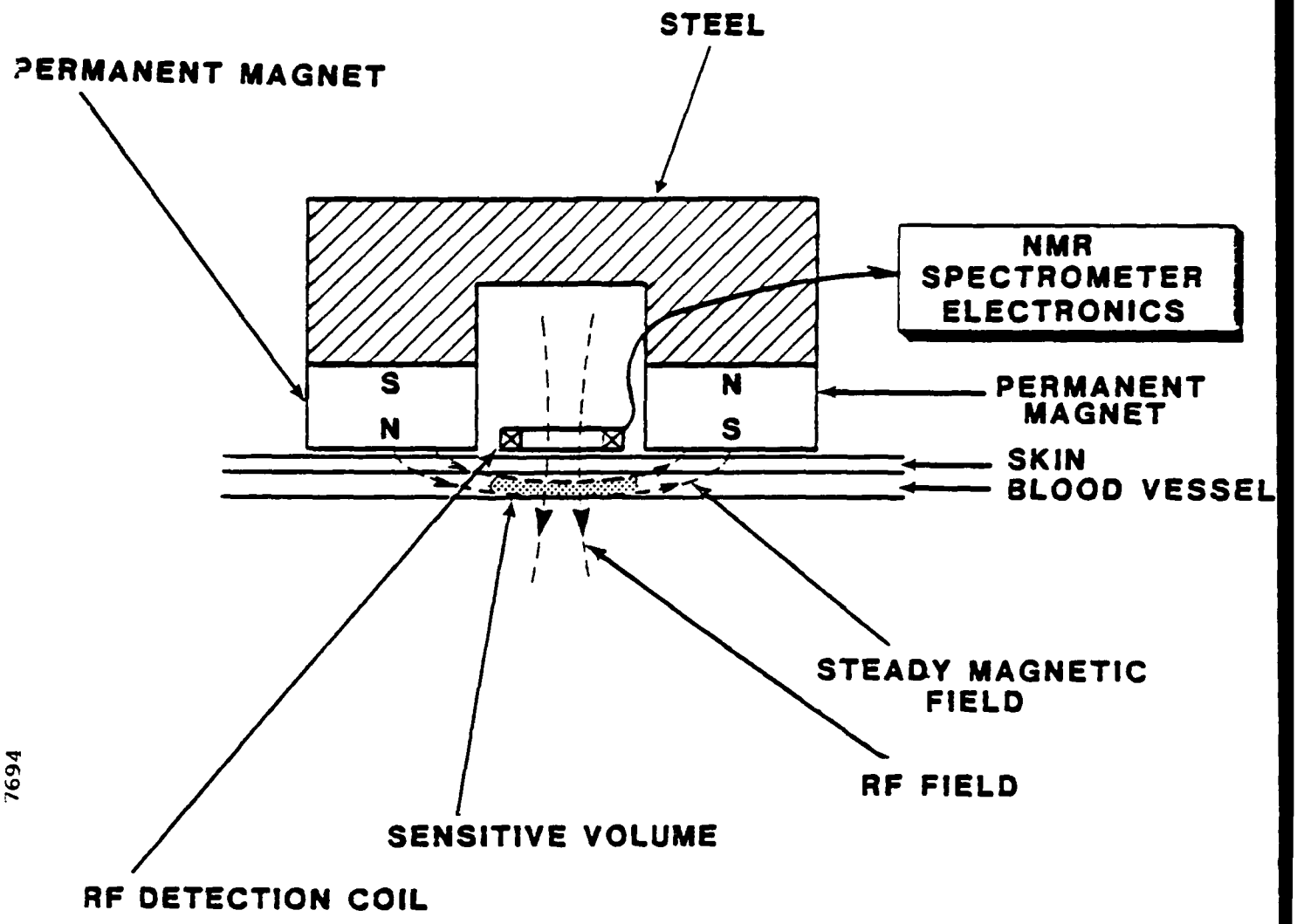

FIGURE 12. BLOCK DIAGRAM OF THE RF DETECTION COIL, THE MAGNET, AND THE NMR SPECTROMETER ELECTRONICS USED TO DETERMINE THE OXYHEMOGLOBIN IN THE BLOOD IN THE BLOOD VESSEL.

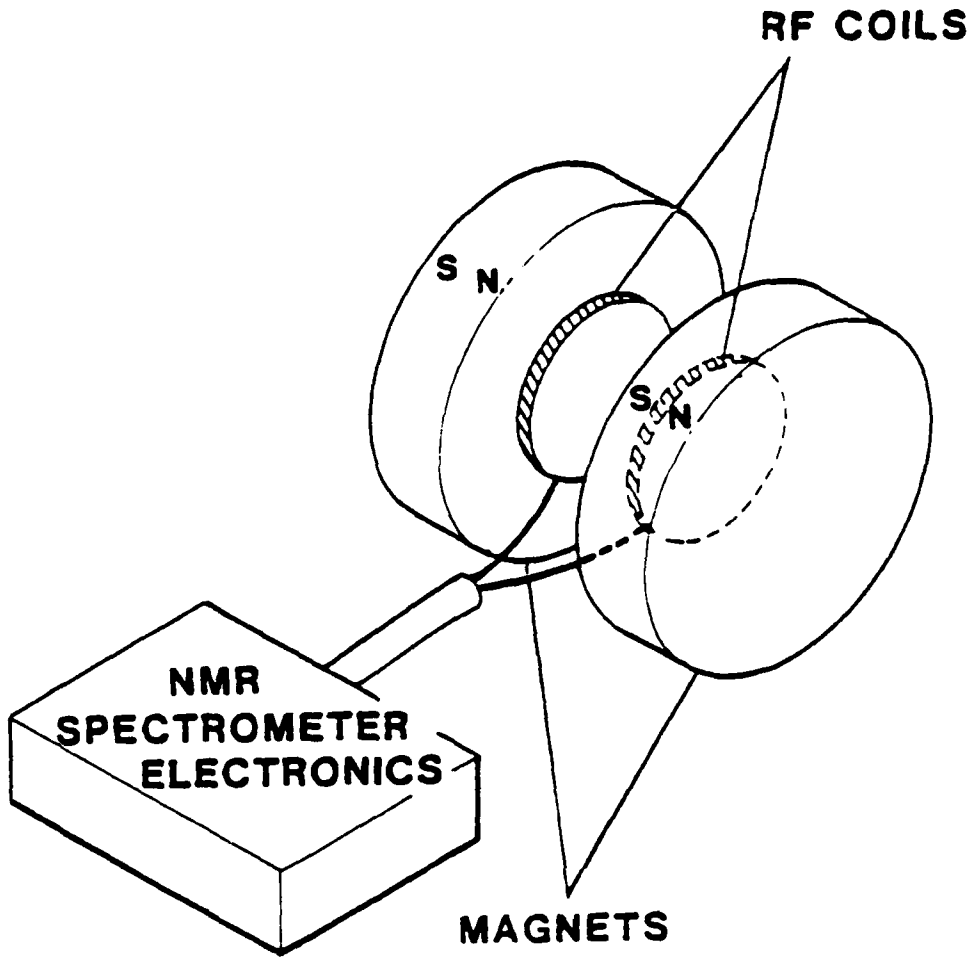

7695

FIGURE 13. BLOCK DIAGRAM OF THE DETECTION COIL, THE MAGNET AND THE NMR SPECTROMETER ELECTRONICS USED TO DETERMINE THE PERCENT OXYHEMOGLOBIN IN THE EAR LOBE OR IN THE FINGER.

cylindrical magnet. The radiofrequency magnetic field $2H_1$ from the two RF coils must be perpendicular to the steady field from the magnets and this can be accomplished by using the bent-head or the surface coil in Figure 11. These types of RF coil are very often used for NMR. With this type of detection head, capillary blood can be measured as well as the arterial or venous blood. In this case, the hydrogen NMR signal from the surrounding tissue should be subtracted from the NMR signal of the tissue plus the blood so that the value of T_2 in the blood can be determined and converted to percent oxyhemoglobin.

V. EXPERIMENTAL PROCEDURES AND RESULTS

A. Performance

The work was performed in four tasks: (1 construction and test of the bubble generator and the NMR detection head (Magnet plus RF coil) to hold the gas bubbles in the blood; (2) hydrogen transient NMR measurements on blood, blood serum, or blood plasma, plus the analysis of the data to determine the values of T_1 and T_2 ; (3) obtain an NMR image of the knee so that the values of T_1 and T_2 of the synovial fluid can be measured; and (4) produce a final report. The work accomplished in each of these four tasks will be described in the following sections.

B. Bubble Generator and NMR Detection Head

In order to make NMR measurements on blood with bubbles of oxygen or nitrogen it is necessary to hold the bubbles motionless for the time required to obtain the transient NMR data from which the values of T_1 and T_2 can be determined. Around one hour was required to take all of the transient NMR data needed to calculate the values of T_1 and T_2. This no-flow condition is needed only for these experiments not for the in-vivo measurements, therefore, the bubble generator had to hold the bubbles relatively fixed inside the detection coil for one hour for the no-flow condition. The no-flow condition had to be used to measure the reference values of T_1 and T_2 for the no-flow condition. To retain the bubbles for an hour in the blood, some means of trapping them had to be used. Thus, the bubble generator needed both a means for making gas bubbles in the blood and a means for trapping them.

After reading the literature and talking to those who had experience in making gas bubbles in blood, it was determined that a Fritted Cylinder type of gas dispersion tube would provide a good source for bubbles of gas in the blood. When some capillary tubes are placed around the inlet tube of the fritted cylinder, the gas bubbles in the blood would be trapped in the capillary tubes and limit their diameter to that of the capillary tubes which were 1.1 to 1.2 mm inside diameter.

The gas dispersion tube and the capillary tubes were ordered and after they were received, several positions of the capillary tubes relative to the fritted glass section of the gas dispersion tube were tried. The position of the capillary tubes shown in Figure 14 was adopted since it produced the desired trapping of bubbles in the blood in the capillary tubes. It was estimated by observation that around 40% of the bubbles in the capillary tubes were sausage shaped, 40% were spherical, while 20% were incomplete bubbles with part of the capillary tube completing the sausage or spherical shape. These shapes were very difficult to observe in water but easy to see in blood.

Containers of oxygen and nitrogen were obtained and fitted with gauges to measure pressure as well as to provide hose connections. The gas chosen, either oxygen or nitrogen, was connected to the bubble generator by means of flexible tubing. The gas dispersion tube with the capillary tubes attached was removed from the test tube and blood was added to the test tube to a depth of 1.5 in. When the gas dispersion tube with the capillary tubes was inserted into the test tube, the blood then covered the bottom 3 in. of the test tube which meant that the blood reached over the top of the capillaries.

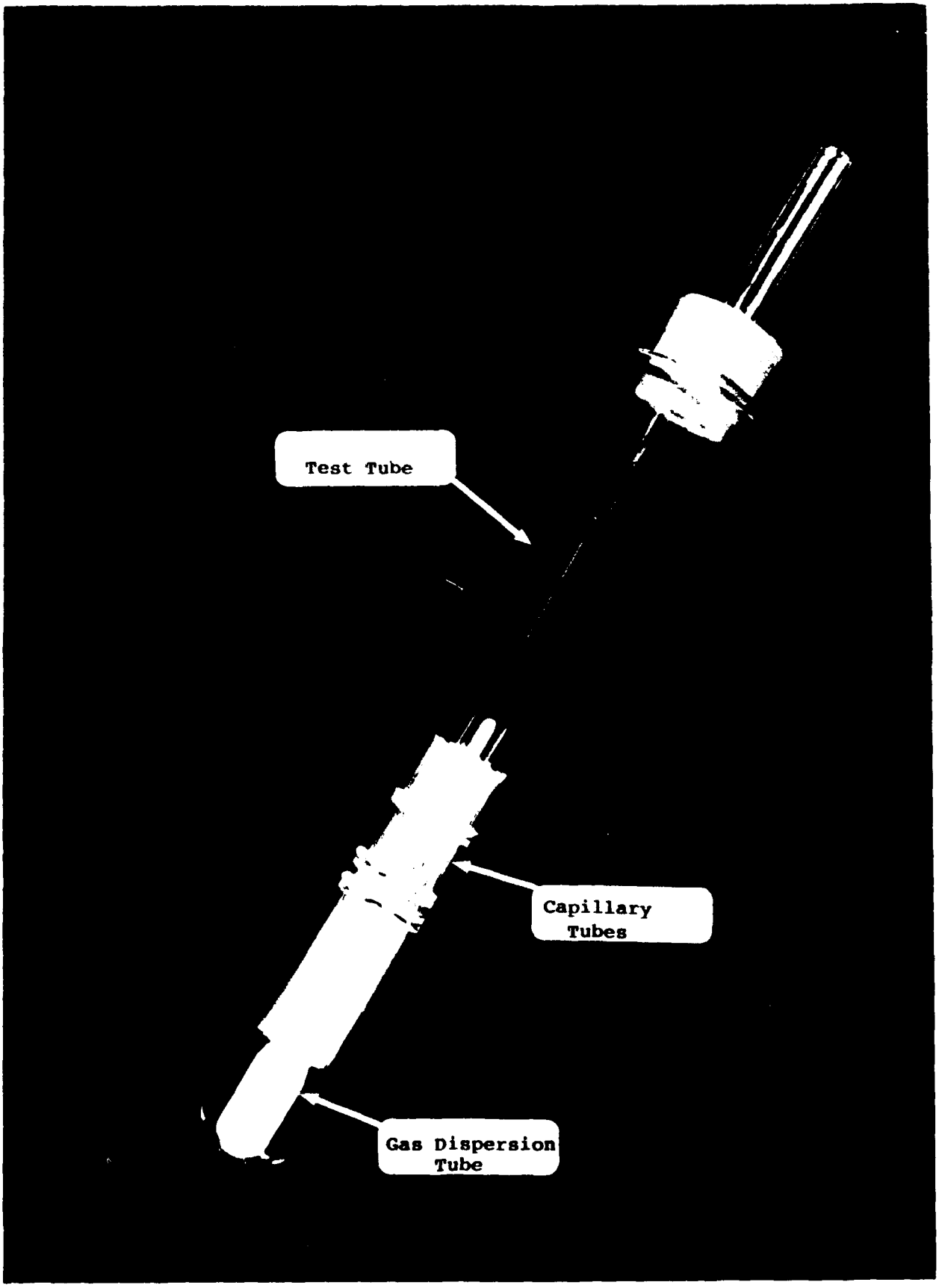

Figure 14. The Bubble Generator Composed of a Gas Dispersion Tube with Capillary Tubes held around the Input Tube of the Gas Dispersion Tube inserted through a Cork into a Test Tube which is 25mm O.D. and 200mm long.

With no gas flowing, the bubble generator with blood in it was inserted into the RF detection coil of the NMR detection head. The hydrogen, free-induction type NMR signal was obtained with the SwRI laboratory NMR spectrometer to check that adequate signal/noise ratio was being obtained to permit NMR data to be taken from which the values of T_1 and T_2 could be determined. To give the values of T_1, a single 90 pulse was used and the repetition rate for the 90 pulse was varied so that the time between pulses varied from values very short compared to T_1 to values three to five times longer than T_1. The peak amplitude of the free induction decay (FID) type of NMR signal was recorded for each value of repetition rate from 50 milliseconds to 8000 milliseconds. When the recorded peak FID amplitude were plotted on semilog graphs, the value of T_1 could be calculated from the slope of the straight line which fitted the data points. The value of T_1 was calculated as the pulse spacing required to reduce the FID peak amplitude to 37% (the value of the exponential when $\tau=T_1$) of the peak amplitude of the FID at a time equivalent to zero pulse spacing. This calculation was accomplished by an analysis program in the HP-1000 computer in Division 15 of SwRI.

The values of T_2 were calculated from a measure of the peak amplitude of the spin-echo which was obtained following a dual-pulse sequence of 90 and 180 pulses separated by a time t_2. The peak of the echo occurs at $2t_2$ and the value of t_2 was varied from values small compared to T_2 to values 2 to 3 times T_2. For most samples, the value of t_2 was varied from 10 milliseconds to 400 milliseconds. When the peak amplitude of the echo was plotted as a function of $2t_2$ on a semilog graph, the value of T_2 is the time when the amplitude of the straight line fitting the data reaches 37% of the value of the straight line at zero time.

C. Samples

Sources were sought for samples of whole blood, blood plasma, blood serum, and synovial fluid. Sources were found for whole blood, blood plasma, and blood serum but no source was found for synovial fluid. It was decided to get whole blood samples since blood plasma and blood serum could be obtained from whole blood. The whole blood samples could not be obtained without heparin added. Therefore, there may be some effect on the relaxation time of the water in the blood caused by the addition of heparin. In the citations from the literature search on NMR measurements in blood, only one[12] was found that discussed the effect of heparin on the spin-lattice relaxation time T_1 for the water in blood. In this reference[12] it was stated; "Little difference in the T_1 values of the packed erythrocytes (from heparinized blood) and of the clot (from spun down nonheparinized blood).". No measurements of T_2 were reported in Reference 12, so the effect of heparin on the value of T_2 in blood is not known.

When experiments were to be made over several consecutive days, the samples of blood used each day were returned to the plastic blood container and stored in the refrigerator each night. In no case was a sample used for more than five consecutive days.

D. Procedure for Obtaining Data and Data Analysis

The hydrogen transient NMR spectrometer at SwRI, a shown in Figure 15, was used to obtain the NMR data from the blood samples. The Bubble Generator in Figure 14 was inserted into the radiofrequency (RF) detection coil which was mounted along with its tuning capacitor between the poles of the magnet shown on the left side of Figure 15. As soon as the RF

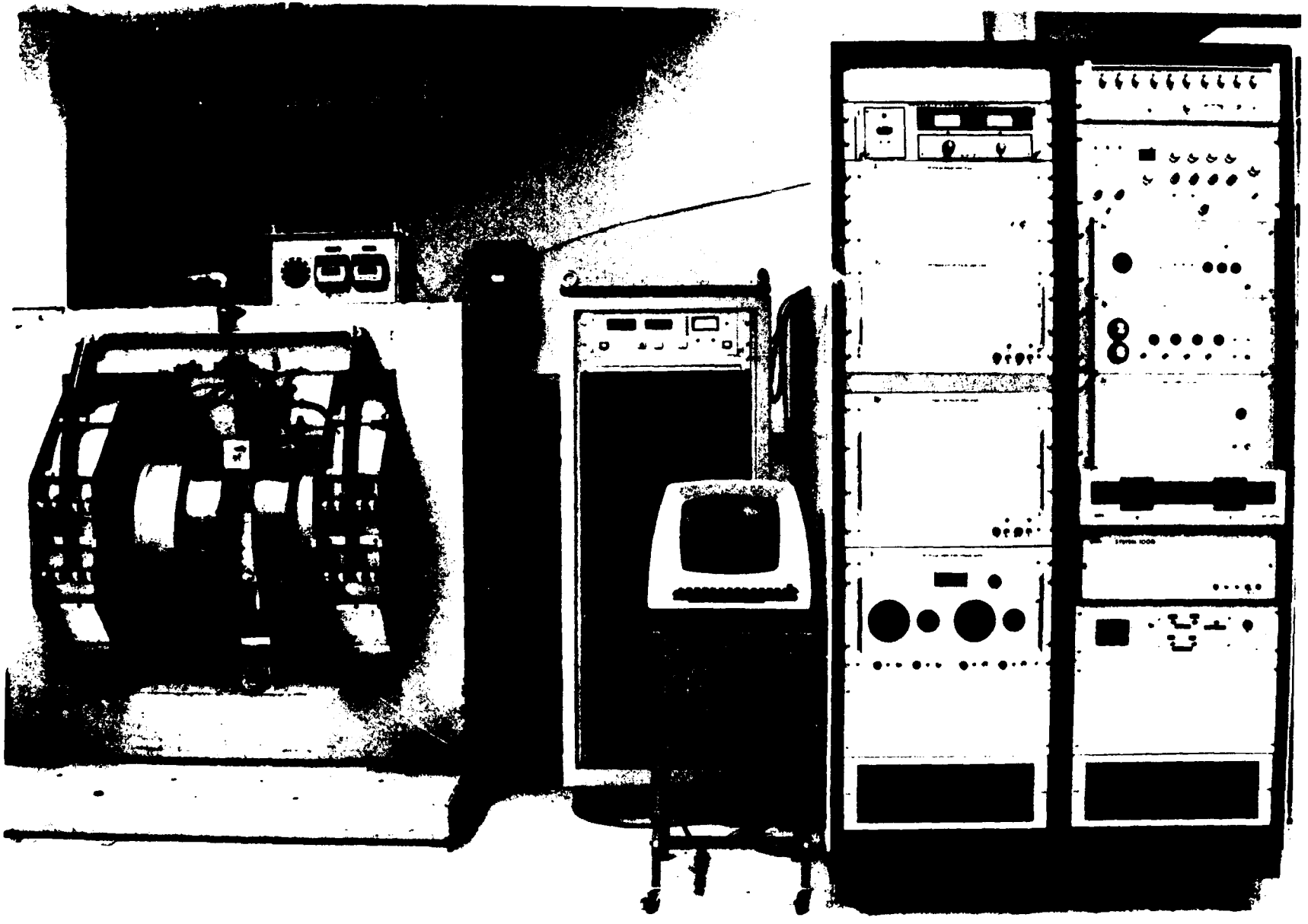

FIGURE 15. A VIEW OF PART OF THE SwRI NMR LABORATORY

detection coil was tuned to resonance at the 27 MHz operating frequency, and the intensity of the magnetic field was adjusted to the value for hydrogen resonance, then the NMR data could be taken for each of the blood samples and conditions used.

The repetition rate method[1] was used to obtain the NMR data from which the values of T_1 were determined. A repeated 90° pulse was used and the peak value of the free induction decay (FID) type NMR signal following the 90° pulse was recorded as a function of the repetition rate which was varied so that the time between the 90° pulses is changed from values which are around $3T_1$ to values which are about $0.1T_1$. The peak FID amplitudes subtracted from the maximum peak FID amplitude are then plotted on semilog axes where the peak FID amplitude is on the log axis (vertical) and the pulse separation time is on the linear axis (horizontal). The semilog graph should be a straight line if there is only one exponential involved. The semilog graph should be a curve if there are two or more exponentials involved. For the data taken from the samples and for the conditions used, all of the graphs from which the T_2 values were calculated, were straight lines which gave one value of T_2 for each sample and each condition. Two examples of the semilog graphs of data, from which the values of T_2 are calculated, are shown in Figures 16a and 16b. The calculation of T_2 begins by fitting a straight line to the graphed data. The value of T_2 is the point on the fitted straight line where the amplitude is $1/e = 0.3679$ times the intercept value A for each straight line. In this case, e is the base of a natural logarithm 2.71828. This point is shown by the dashed lines in Figures 16a and 16b.

The graphed data from which the T_1 values were calculated gave some straight lines and some curves. Thus, for some samples there was one value of T_1 and for other samples there were two values of T_1: T_{11} and T_{12}. For the single line fit, the single value of T_1 is calculated in the same manner as the single value of T_1. An example of the semilog graph of the NMR data having a single value of T_1 is given in Figure 17. Again the graphed data is fitted by a single straight (solid) line. The dashed lines in Figure 17 identify the coordinates of T_1.

An example of the semilog graph of a dual exponential curve from which two values of T_1 can be calculated is given by the data points in Figure 18a. The procedure for the deconvolution of the curve is first to fit with a solid straight line the data at the long values of time (data points 9 through 15 in Figure 18a). The dashed lines in Figure 18a indicate the value of T_{12} to be equal to 1361 milliseconds, the longest of the two values. The first straight line fitted to data points 9 through 15 is then subtracted from the curve represented by the data points 1 through 15. The results of the subtraction is given by the data points 1 through 9 graphed in Figure 18b. When the second straight line is fitted to the subtracted values for data points 1 through 9, the value of T_{11}, the shortest value, can be determined at the 36.79 percent point as indicated by the dotted line in Figure 18b to be T_{11} = 459 milliseconds.

Division 15 of the Southwest Research Institute has the analysis process described above as a program in their HP-1000 computer. The program uses a menu system whereby the operator enters the data from a disc used to record the data as it was taken from the SwRI/NMR Spectrometer by the computer (PDP 11/03) shown in Figure 15 in the middle of the rack on the extreme right. After the data is entered, the analysis program presents a graph on the CRT screen of the data set desired to be analyzed. The menu then asks which points should be fitted by the first straight line. The first fitted line is then drawn on the graph

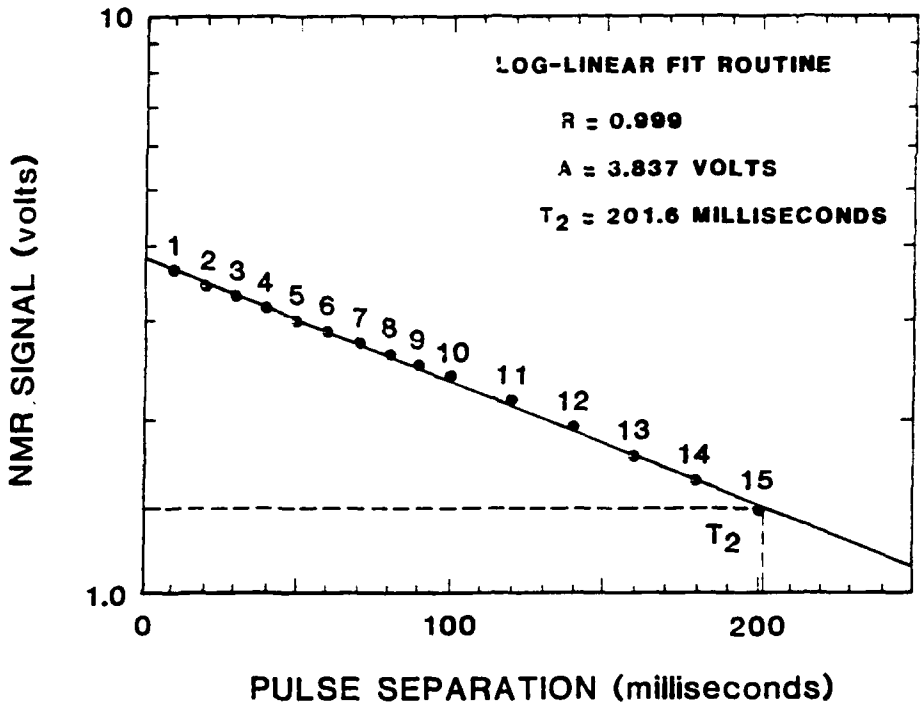

FIGURE 16A. LOG LINEAR GRAPH OF THE NMR DATA FITTED BY A STRAIGHT LINE FROM WHICH THE VALUES OF THE INTERCEPT A AND THE SPIN-SPIN RELAXATION TIME T_2 CAN BE CALCULATED FOR ONE BLOOD SAMPLE (# 26 IN TABLE I).

7697

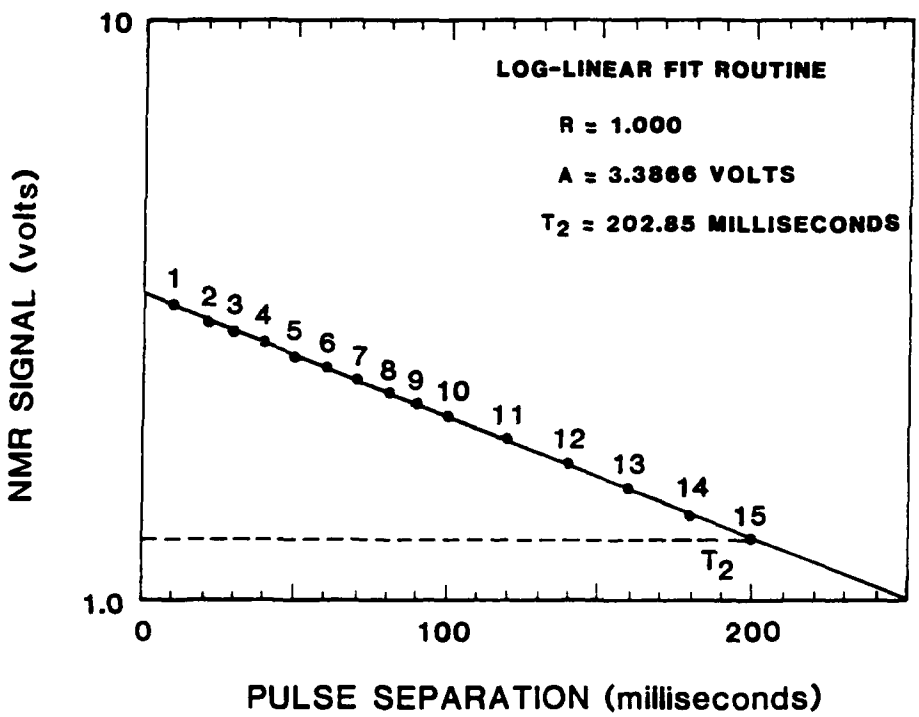

FIGURE 16B. LOG LINEAR GRAPH OF THE NMR DATA FITTED BY A STRAIGHT LINE FROM WHICH THE VALUES OF THE INTERCEPT A AND THE SPIN-SPIN RELAXATION TIME T_2 CAN BE CALCULATED FOR A SECOND BLOOD SAMPLE (# 25 IN TABLE I).

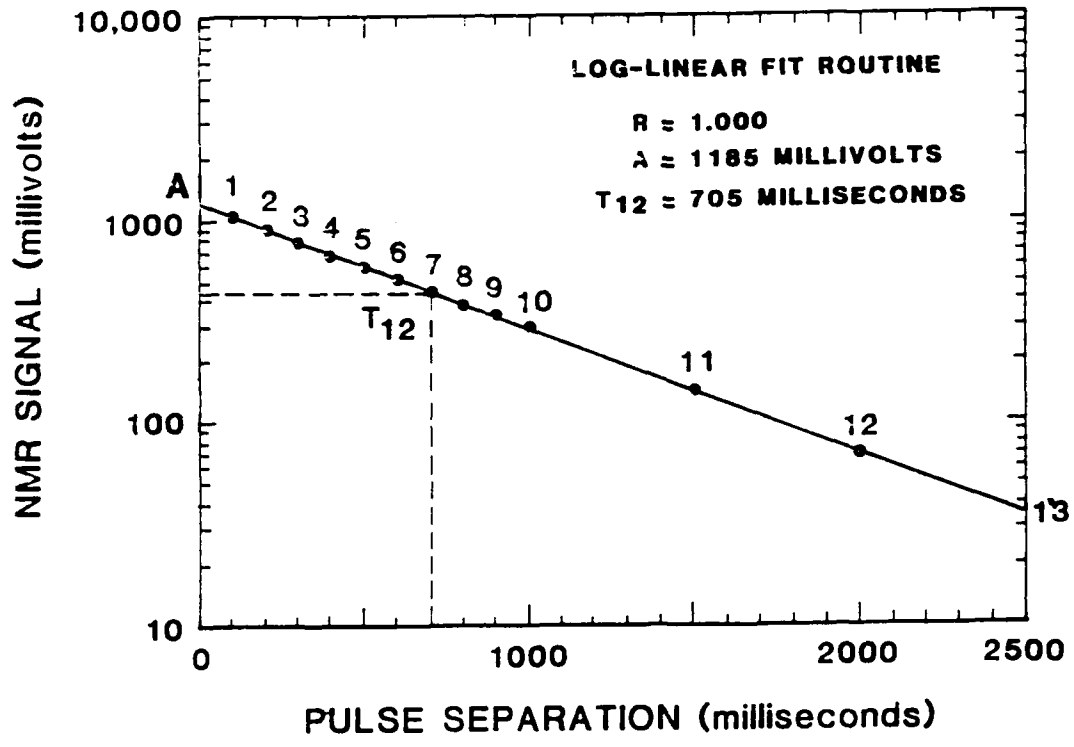

7698

FIGURE 17. EXAMPLE OF A SINGLE STRAIGHT LINE FIT TO THE SPIN-LATTICE RELAXATION TIME NMR DATA FROM WHICH A SINGLE INTERCEPT VALUE A AND A SINGLE T_{12} VALUE WAS CALCULATED FOR BLOOD SAMPLE NO. 22 IN TABLE I.

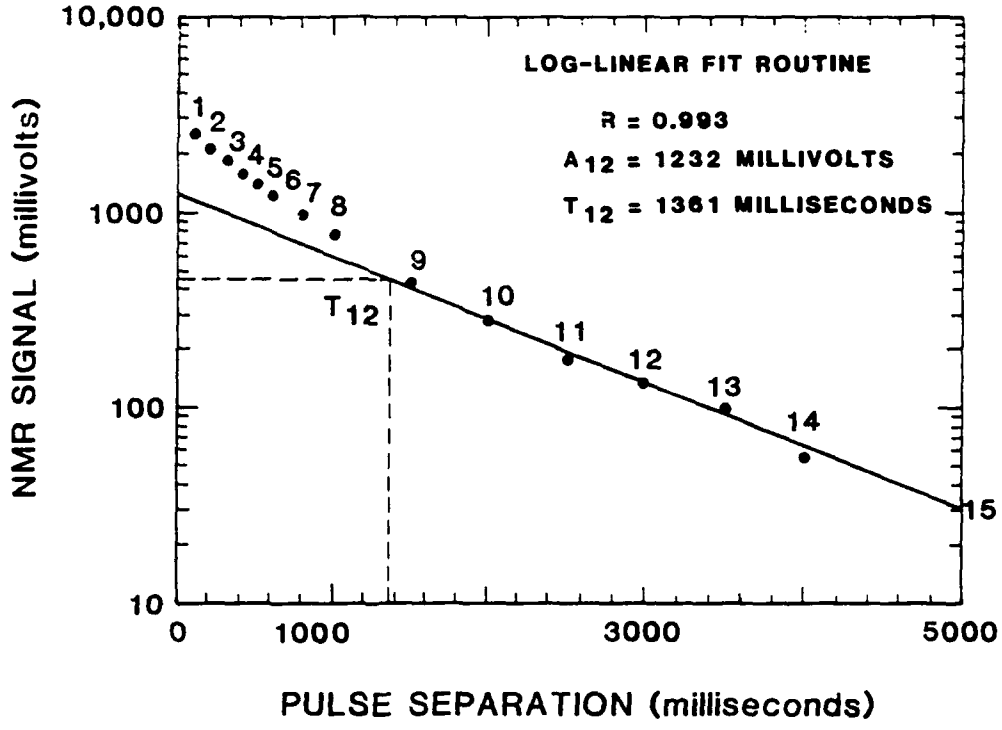

FIGURE 18A. LOG-LINEAR GRAPH OF THE NMR DATA FITTED THROUGH THE FIRST STRAIGHT LINE THROUGH POINTS 9 THROUGH 15 FROM WHICH THE VALUES OF THE INTERCEPT A_{12} AND THE LONGEST VALUE OF THE SPIN-LATTICE RELAXATION TIME T_{12} CAN BE CALCULATED FOR SAMPLE NO. 20 IN TABLE I.

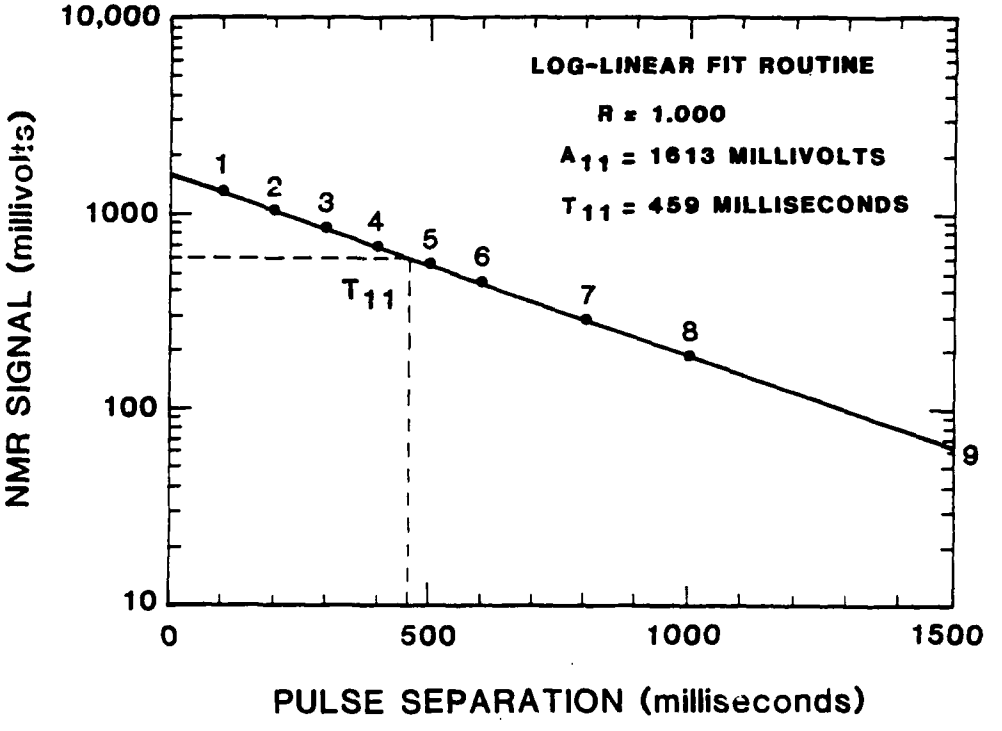

FIGURE 18B. LOG-LINEAR GRAPH OF THE DIFFERENCE BETWEEN THE CURVE OF THE DATA IN FIGURE 18A AND THE FIRST STRAIGHT LINE FIT ALSO IN FIGURE 18A. THE REMAINING DATA POINTS ARE NUMBERS 1 THROUGH 9 WHICH CAN BE FITTED BY THE SECOND STRAIGHT LINE FROM WHICH THE VALUES OF THE SECOND INTERCEPT A_{11} AND THE SECOND (SHORTEST) SPIN-LATTICE RELAXATION TIME T_{11} CAN BE CALCULATED FOR SAMPLE NO. 20 IN TABLE I.

and the values of the confidence factor, the zero intercept value A and the values of T_2 or T_1 for that fitted line are displayed on the screen. The analysis program then subtracts the first straight line from the data points and presents a graph on the screen if the difference or remainder is significant. For significant differences the menu again asks which points are to be fitted by the second straight line. The menu will keep on with this process until the last subtraction gives an insignificant difference. The analysis then displays on the last significant graph, the confidence factor, the zero-intercept value and the relaxation time for each straight line needed to completely deconvolute the graph of the data.

One set of experiments were made with the blood bubbled with oxygen, bubbled with air, bubbled with nitrogen, and vacuum degassed. At first, the blood was bubbled in the Bubble Generator when it was outside of the NMR detection head. The Bubble Generator with the gas bubbles and the blood in the capillary tubes was placed into the NMR detection coil, the NMR data was taken, and the values T_{11}, T_{12}, and T_2 were determined as described above. In these first measurements, there was little movement of the bubbles or of the blood in the Bubble Generator while the NMR measurements were made. About one hour was required to obtain and check all of the NMR measurements. One to one and one-half hours were required to clean the Bubble Generator, after one series of NMR measurements were made on one sample with one type of gas bubbles. Then, a second sample of blood could be placed in the Bubble Generator and bubbled with another gas. Considering the times for cleaning, changing blood samples producing the gas bubbles, and obtaining the NMR data, three to four hours were required for each sample so that on most days 2 samples could be measured. Once in a while three could be completed. The blood samples were obtained from blood banks. One pint of blood could be used for several days when the blood was stored in a refrigerator.

The main experimental objective of the proposed program was to perform the NMR measurements on oxygenated blood, nitrogenated blood, degassed blood, and blood loaded with expired air. The color of the blood was used to determined when the blood was oxygenated (red color) and when it was deoxygenated (black-red color). There are other measurements which we would like to have: Ph, CO_2, percent oxyhemoglobin, etc. However, the available funds would not permit these measurements, especially since the time to perform one series of NMR measurements on one sample was three to four hours as described above.

The second experimental objective is to test the effect of the flow of the gas bubbles on the NMR data. In the literature on the NMR measurements of flow it is stated that the line width of the NMR absorption curve increases with the flow rate, that is $\Delta\omega = kq$, where k is the constant and q is the flow rate. This means that since the spin-spin relaxation time is equal to $2/\Delta\omega$, that is $T_2 = 2/\Delta\omega$, and since $\Delta\omega = kq$, then $T_2 = 2/kq$ and T_2 decreases as the flow rate increases. It is also stated[13] that the value of T_2 is also inversely proportional to the flow rate. Thus for a flowing liquid, both T_2 and T_1 should decrease as the flow rate increases. No one has written in the literature about the effect on T_1 and T_2 of the flow rate of gas bubbles in a liquid where there is an interaction between the gas and the liquid which also may change the relaxation times T_1 and T_2 of the liquid. There was also nothing found in the literature about the effect of the flow of both the fluid and the bubbles, where each may be moving at different rates and in different directions. While an exhaustive study of the effect of the flow of bubbles and blood was beyond the scope of the proposed program, it was possible on a few samples to determine the differences in T_1 and T_2 from blood with fixed bubbles and blood with moving bubbles. Therefore, a few measurements were made both with fixed bubbles and with moving bubbles.

E. Results

Most of the NMR measurements were made on blood samples under different conditions. Two NMR measurements were made on distilled water, one where the water was degassed and one where the water was filled with oxygen. Two NMR measurements were made with blood plasma: one degassed and one with oxygen. Four of the measurements were made with fresh blood from a volunteer. The listing of the values of T_2, T_{11} and T_{12} ($T_{12} > T_{11}$) for the samples and conditions used are given in Table I. In the list, some of the blood samples were bubbled with oxygen and with nitrogen, while some were tonometered (placed under gas pressure) with oxygen and nitrogen. Also in the list, some measurements were made only to obtain the value of T_2 in order to reduce the measurements time so as to limit any changes with time in the blood samples 1 through 4 and 24 through 26 listed in Table I.

It can be observed in Table I that all of the samples had only one value for the spin-spin relaxation time T_2. The mean value for all the T_2 values is 180.71 milliseconds with a standard deviation of 57.96 milliseconds which is 32 percent of the mean.

Most of the samples gave dual values for the spin-lattice relaxation times (T_{11} and T_{12}, where $T_{12} > T_{11}$). Samples 5, 11, 17, 18, 21, 22, 27, and 28, all had recorded only the longest values of the spin-lattice relaxation time T_{12}. No T_{11} or T_{12} values were obtained for samples 1, 2 3, 4, 24, 25, and 26 because the NMR data from which they could be determined was not taken in order to reduce the measurement time and the change in the sample over the measurement period. The mean of the T_{12} (longer) values measured is 1242 milliseconds with a standard deviation of 480 milliseconds which is 38.6 percent of the mean. The mean of the T_{11} (shorter) values is 358 milliseconds with a standard deviation of 79 milliseconds which is 22 percent of the mean. The mean of T_{11} was obtained from 21 values while the mean of T_{12} was determined from 13 values. T_{11} and T_{12} values from the two water samples (27 and 28) were not included. It should also be observed from Table I that both of the spin-lattice relaxation times (T_{11} and T_{12}) for each of the blood samples are longer than the value of T_2. A comparison of the relative values (T_{11} and T_{12} compared to T_2) with the graph in Figure 3 will indicate that: (1) there are two binding states for water in blood, (2) the binding in each of the two states is relatively strong compared to that of distilled water (No. 28 in Table I), (3) all of the water in whole blood is bonded; none of the water is free, and (4) the water in the degassed plasma has only one value of the spin-lattice relaxation time (T_{12}) which is similar to the longest value T_{12} for whole blood. It should also be noticed that the value of T_{12} for the plasma of 385 milliseconds is more than twice the mean value of 180.71 milliseconds for T_2 in blood.

Two measurements are shown in Table I of the T_2 and T_{12} values for degassed distilled water and distilled water with oxygen bubbles. In both cases, the values of T_2 and T_{12} are equal as would be expected from the graph in Figure 3. From the graph in Figure 4, it is expected that the values of T_{11} and T_2 would decrease as the oxygen concentration increased. The values for T_{12} and T_2 in Table I for the two samples of water, with and without dissolved oxygen, are smaller for the water with oxygen (1050 milliseconds) than for the water without oxygen (2400 milliseconds). It should be noted that the measurement frequency for the data graphed in Figure 4 is 6 MHz, while the measurement frequency for the data in Table I is 27 MHz. The values of T_1 increase as the measurement frequency increases as shown by the graph in Figure 3. The data in reference 7 were taken at 6 MHz and the values for T_1 are given in Table II.

TABLE I

Values of T_2, T_{11}, and T_{12} for All Samples

Sample	Condition	T_2 (ms)	T_{11} (ms)	T_{12} (ms)
1	Oxygenated blood (artery)	115	--	--
2	Nitrogen-filled blood	70	--	--
3	Blood from vein	76	--	--
4	Blood with oxygen bubbles	103	--	--
5	Degassed plasma	385	--	1432
6	Blood bubbled with air	160	376	1511
7	Blood bubbled with oxygen	148	309	1420
8	blood bubbled with nitrogen	116	412	1515
9	Blood bubbled with expired air	152	429	1766
10	Blood tonometered with nitrogen	144	419	1002
11	Blood tonometered with oxygen	201	--	874
12	Blood tonometered with air	193	427	962
13	Blood bubbled with expired air	180	330	971
14	Blood bubbled with room air	151	231	942
15	Blood bubbled with oxygen	132	181	839
16	Blood bubbled with nitrogen	173	372	1049
17	Oxygenated blood, flowing bubbles	269	--	1229
18	Deoxygenated blood	233	--	1163
19	Nitrogen bubbled blood	133	396	1275
20	Vacuum degassed blood	155	459	1361
21	Oxygen bubbled blood	140	311	2873
22	Oxygen bubbled blood	154	--	705
23	Oxygen bubbled blood	--	--	705
24	Nitroten tonometered blood	172	--	--
25	Oxygen tonometered blood	203	--	--
26	Vacuum degassed blood	202	--	--
27	Distilled water bubbled with oxygen	1050	--	1050
28	Degassed distilled water	2400	--	2400
	Mean Value for Blood	180.71	358	1242
	∂ Value for Blood	57.96	79	480

TABLE II

Values of T_1 for Blood (Ref. 7 and 1-5 of Table I)

Sample	(Ref. 7) T_{12} (msec)	SwRI T_2 (msec)	T_{12} Values at SwRI
Venous Blood	599	76	mean = 1187, σ = 193
Arterial Blood	559	115	mean = 1024, σ = 279
Deoxygenated Blood	1171	385	1432
Oxygenated Blood	1098	--	--
Blood-Bank Blood	1744	--	mean = 1187, σ = 193

No values for T_2 were mentioned in Reference 2. In order to reduce the measurement time for the samples similar to those in Reference 7, only the values of T_2 were determined. Therefore, in Table II, no values of T_1 for these four samples are given. What is listed in Table II are the mean values of the longest spin-lattice relaxation time, T_{12}, for all the blood samples for which the spin-lattice relaxation time values were measured.

The fresh blood from the volunteer was used to obtain the values of T_2 from four blood conditions: (1) as-received arterial blood, (2) blood with oxygen bubbles, (3) as-received venous blood, and (4) blood with nitrogen bubbles. Only the NMR data needed to determine the values of T_2 was taken from the above four samples in order to reduce the changes taking place in the blood with time. The four values of T_2 were entered into the graph in Figure 19 of T_2 versus percent oxyhemoglobin using the fitted line from Figure 10. No measurements of percent oxyhemoglobin were made on these four samples or any of the samples because no sensor was available for this measurement on the samples in the NMR detection head except for the change in color (red to dark blue or black). In Figure 19, the horizontal lines represent the values of T_2 for each condition. Where these lines cross the curve in Figure 19 should give the value percent oxyhemoglobin for the three conditions. The order of the values of T_2 in Figure 19 is the same as that anticipated from Figure 10 (Reference 12). Arterial blood should have a higher value of T_2 than the blood with oxygen bubbles. The venous blood should have the next lowest value of T_2 while nitrogen bubbled blood should have the lowest value of T_2. The hydrogen transient NMR measurements for these four conditions in fresh blood should be repeated for a statistically valid number of samples so that the mean, standard deviation, and range can be determined. The data graphed in Figure 10 shows a small range of T_2 for each value of percent oxyhemoglobin but more measurements are needed. More NMR measurements also will need to be made coupled with a determination of percent oxyhemoglobin while the sample is being measured in the NMR detection head for both stationary and flowing gas bubbles. These measurements of T_2 will also need to be repeated for both stationary and flowing blood. They will also need to be repeated for fresh blood and for Blood-Bank samples with heparin.

The results in Table I can be separated into five categories of non-flowing gas conditions: (1) blood tonometered or bubbled with air, (2) blood tonometered or bubbled with oxygen, (3) blood tonometered or bubbled with nitrogen, (4) blood bubbled with expired air, and (5) vacuum degassed blood. The comparison of the values of T_2 for blood in the five, non-

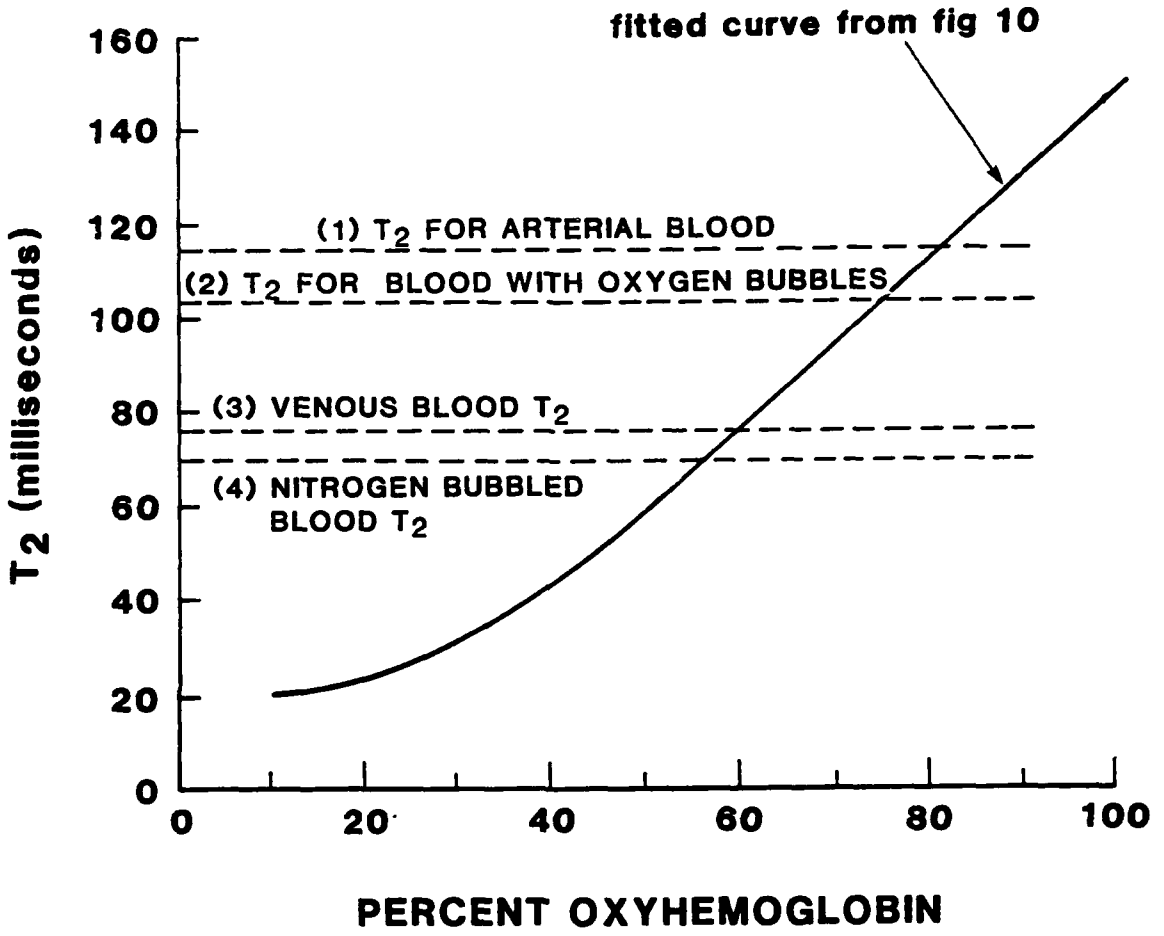

FIGURE 19. THE T_2 VALUES SHOWN ON THE GRAPH OF T_2 VERSUS PERCENT OXYHEMOGLOBIN FROM FIGURE 10 FOR FOUR CONDITIONS IN THE FOUR FRESH BLOOD SAMPLES: (1) ARTERIAL BLOOD, (2) ARTERIAL BLOOD WITH OXYGEN BUBBLES (NO FLOW), (3) VENOUS BLOOD, AND (4) BLOOD WITH NITROGEN BUBBLES.

flowing gas conditions are listed in Table III. In two conditions, (oxygen tonometered or bubbled and nitrogen tonometered or bubbled), the bubbles were allowed to flow. The comparison of the T_2 values for the two flowing-bubble conditions can be made from the data listed in Table IV. The mean values of T_2 for the five non-flowing conditions are graphed in Figure 20. The mean values of the two flowing conditions are also graphed in Figure 20. The mean values of the two flowing conditions are also graphed in Figure 20. When the data in Figure 20 is compared with that in Figure 19, it can be concluded that the two mean values of T_2 for the two gas conditions with flow are much longer than the mean values of T_2 for the five gas conditions without flow. It can also be concluded that the mean values of T_2 for the five gas conditions in blood-bank blood without flow are larger than the T_2 values from the four gas conditions in Figure 19 when fresh blood was used. We have concluded that there was some difference between the fresh blood and the blood from the blood bank. We have also concluded that the flow of gas bubbles will have some influence to lengthen the value of T_2 so that some correction for the flow of gas bubbles may need to be made. Follow-on work should contain measurements of the Ph and percent oxyhemoglobin for the blood in the NMR detection coil as well as the effects of Heparin on the blood relaxation times T_2, T_{11}, and T_{12}.

The last data to be collected were the relaxation times T_1 and T_2 of the synovial fluid and the Magnetic Resonance Image (MRI) of the knee using the Siemens Magnetic Resonance Imager in the Southwest Methodist Hospital. Time on the Siemens MRI unit was unavailable except for an hour at 0700 on 30 September 1986. The SwRI project manager volunteered the use of his own knee but the MRI equipment malfunctioned and the measurement was reset for late in November 1986.

Attempts were made to obtain synovial fluid so that the values of T_1 and T_2 could be determined for this fluid both with and without bubbles. But no source of synovial fluid was found and it was decided to use the ability of the Siemens MRI unit to determine the values of T_1 and T_2 for the synovial fluid in the knee at the same time that the Magnetic Resonance Image of the knee was being made. The staff of the Radiology Department of the Southwest Methodist Hospital were very eager to determine this relaxation time since it would be the first time that this feature of the Siemens MRI had been used.

The four Magnetic Resonance Images of the knee, in Figures 21 and 22, were used to obtain not only the images but also two values of T_1 and T_2 in the synovial fluid. There are two images shown in each of Figures 21 and 22. In each of the two images in Figure 21 and Figure 22, there is a small square under the Patella in the Bursa under Quadriceps femoris[14] which is the synovial membrane. This synovial membrane of the knee joint is the largest and most extensive in the body.

Each of the two pictures in Figures 21 and 22 is an image of a sagittal slice through the knee. Each image is an image of the density of the hydrogen nuclei called a spin density map. In Figure 21a (top), the image has been T_2 weighted so that the NMR signal from the area defined by the square can be used to calculate the value of T_2. The image in Figure 21b (bottom) has been T_1 weighted so that the NMR signal from the square can be used to calculate the value of T_1). Because of the above different weighting, the two images in Figure 21 appear different. The same is true for the two magnetic resonance images in Figure 22. The values of T_1 and T_2 obtained from the synovial fluid in the bursa below the Patella are given in Table V. For the two images in Figure 22, the variables L1, CO, and TR are slightly different from those in Figure 21. It is planned in the follow-on work that the

TABLE III

T_2 Values for Blood in Five Non-Flowing Gas Conditions

Gas Condition	T_2 Values	
	Mean	Standard Deviation
(1) Oxygen tonometered or bubbled	155	24
(2) Air tonometered or air bubbled	168	18
(3) Expired air bubbled	166	14
(4) Nitrogen tonometered or bubbled	148	22
(5) Vacuum degassed	155	--

TABLE IV

T_2 Values for Blood in Two Flowing Gas Conditions

Gas Condition	T_2 Values	
	Mean	Standard Deviation
(1) Flowing oxygen bubbled	251	18
(2) Flowing nitrogen bubbled	202.5	0.5

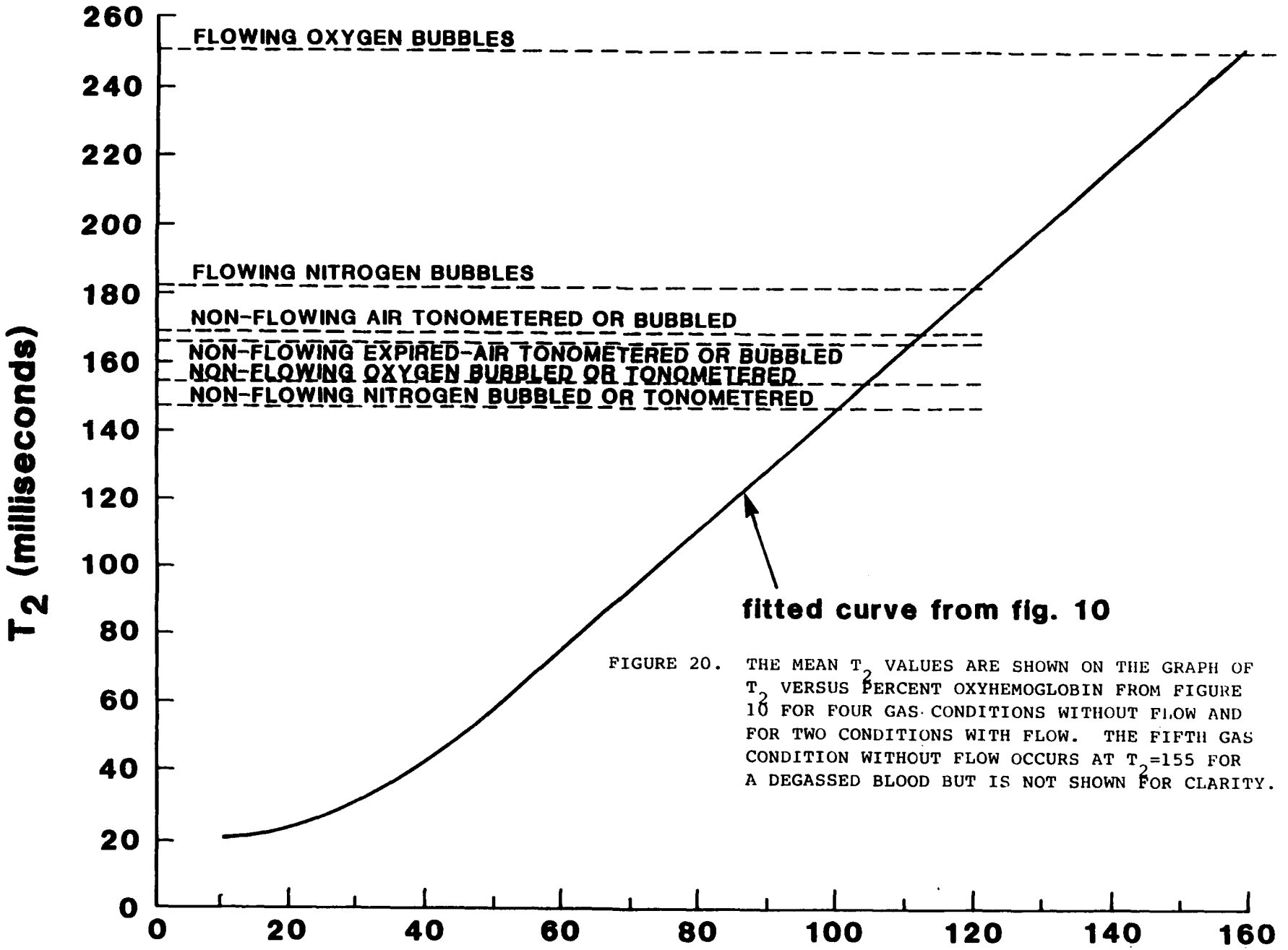

FIGURE 20. THE MEAN T_2 VALUES ARE SHOWN ON THE GRAPH OF T_2 VERSUS PERCENT OXYHEMOGLOBIN FROM FIGURE 10 FOR FOUR GAS CONDITIONS WITHOUT FLOW AND FOR TWO CONDITIONS WITH FLOW. THE FIFTH GAS CONDITION WITHOUT FLOW OCCURS AT T_2=155 FOR A DEGASSED BLOOD BUT IS NOT SHOWN FOR CLARITY.

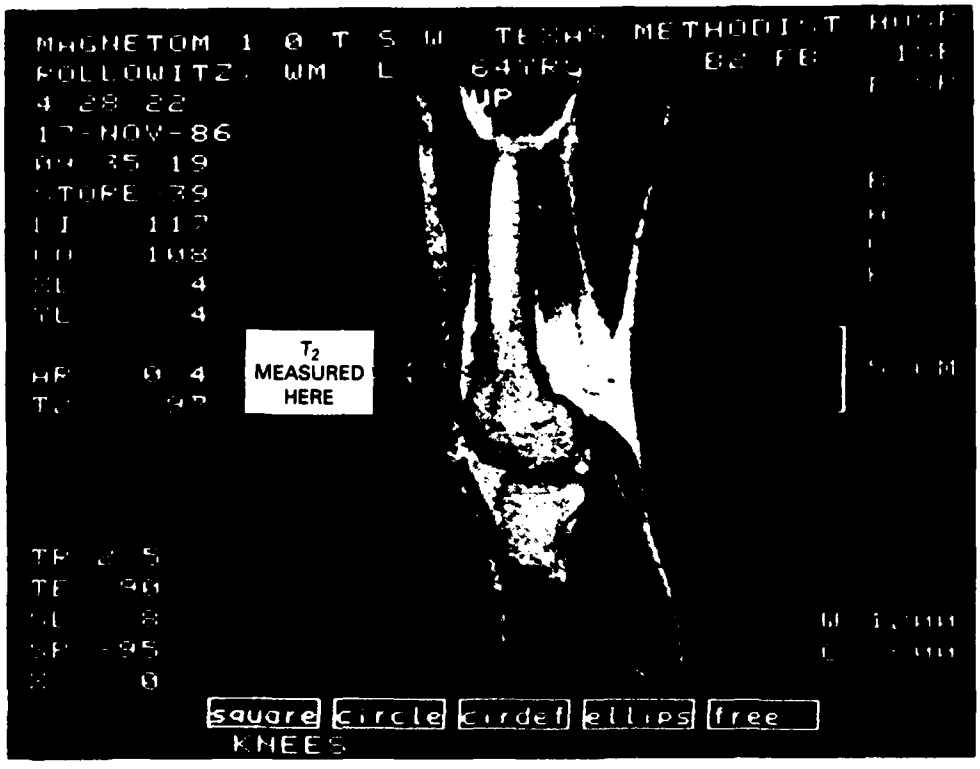

T_2
(a) MEASUREMENT
T_2 WEIGHTED

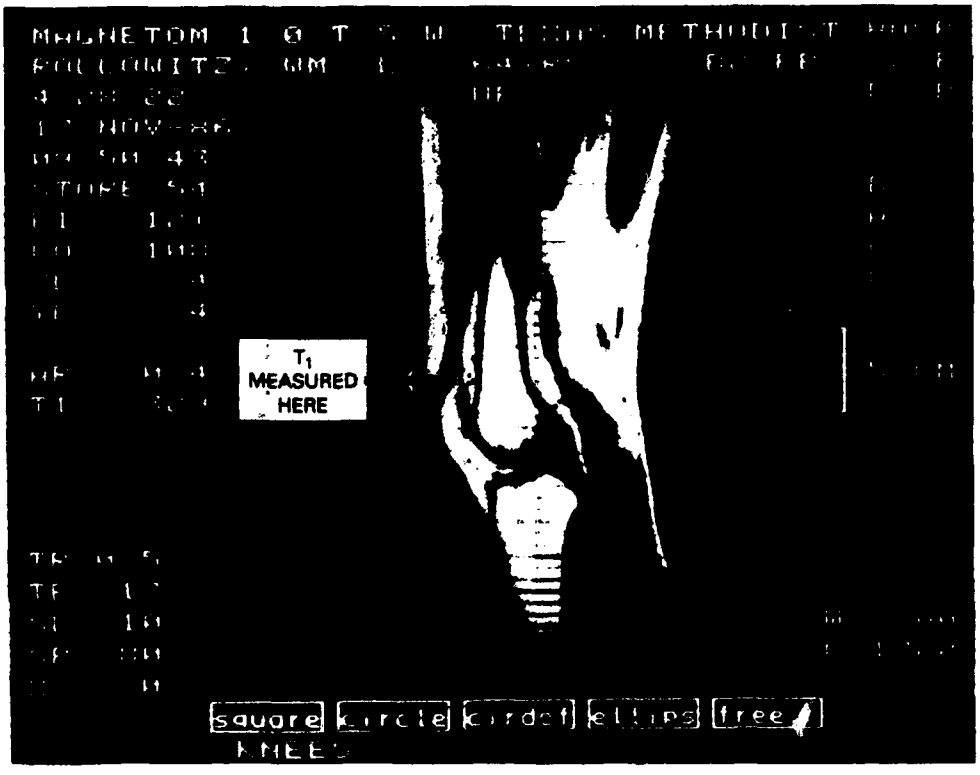

T_1
(b) MEASUREMENT
T_1 WEIGHTED

Figure 21. Magnetic Resonance Image of the Knee (Sagital)
(a) The T_2 weighted image is used to determine the value of T_2.
(b) The T_1 weighted image is used to determine the value of T_1.

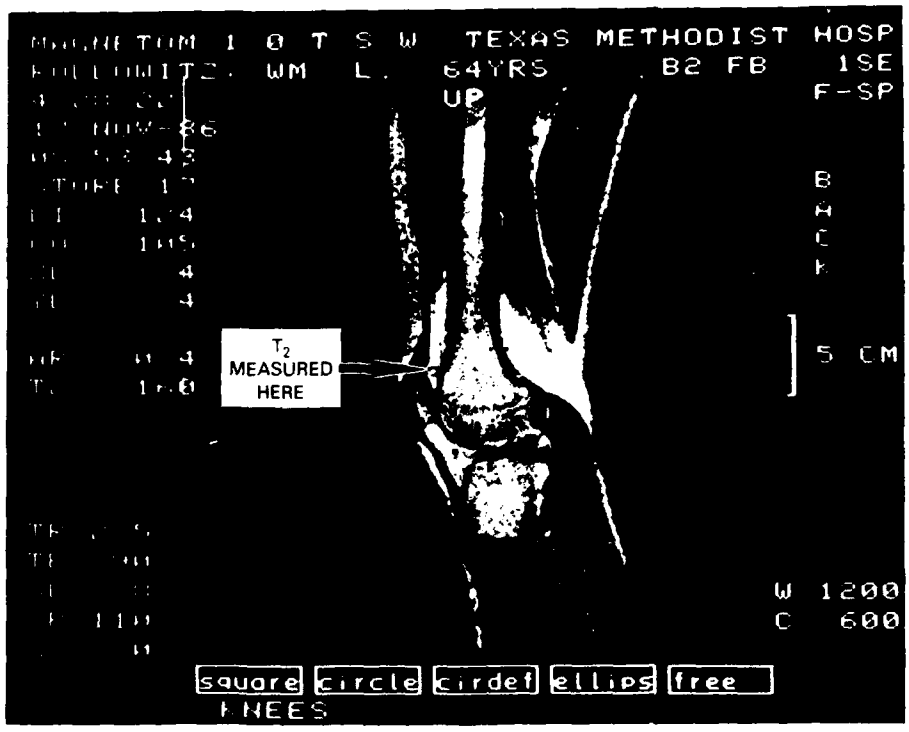

T_2
(a) MEASUREMENT
T_2 WEIGHTED

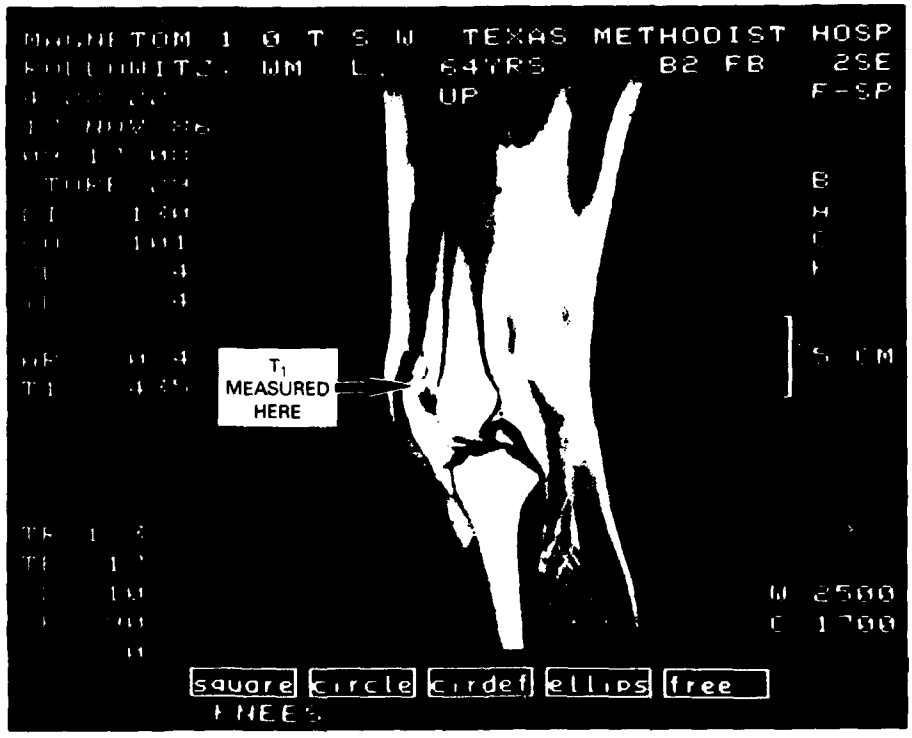

T_1
(b) MEASUREMENT
T_1 WEIGHTED

Figure 22. Magnetic Resonance Image of the Knee (Sagital) with different values of L, CO, and TR from those in Figure 21 and at slightly different positions in the synovial membrane.
(a) The T_2 weighted image is used to determine the value of T_2.
(b) The T_1 weighted image is used to determine the value of T_1.

values of T_1 and T_2 be determined in an in-vitro sample of synovial fluid with no oxygen bubbles, with bubbles of oxygen and with bubbles of nitrogen if a source of synovial fluid can be found

TABLE V

Relaxation Time Values T_1 and T_2 in the Synovial Fluid

Figure No.	T_1 (ms)	T_2 (ms)
21	329	97
22	435	160

VI. CONCLUSIONS AND RECOMMENDATIONS

A. Conclusions

The main objectives of the proposed program were successfully completed. The objectives were to perform the NMR measurements on oxygenated blood, nitrogenated blood, degassed blood, and blood loaded with expired air, and to obtain a magnetic resonance image (MRI) of the knee. As can be concluded from Table I, NMR measurements were made on sixteen samples of oxygenated blood. The oxygen was put into the blood in the form of non-flowing oxygen bubbles, non-flowing air bubbles, flowing oxygen bubbles, oxygen under pressure (tonometered), and non-flowing bubbles of expired air. NMR measurements were made on six samples of blood with nitrogen in the form of non-flowing nitrogen bubbles, flowing nitrogen bubbles, and nitrogen under pressure (tonometered). NMR measurements were made on three samples of degassed blood, on one sample of degassed plasma, one sample of degassed water, and one sample of water with oxygen bubbles. One sample of oxygenated plasma was also measured with the NMR equipment at SwRI but no data was obtained because of a malfunction. It could not be repeated. The NMR measurements were made with the NMR equipment shown in Figure 15. Modifications were made to the detection head to accept the bubble generator, shown in Figure 14, which was constructed during the program.

It was concluded from the T_1 and T_2 measurements that there was only one value of T_1 for each of the blood samples measured while there were two values of T_2, (T_{21} and T_{22}), for each blood sample. There was only one value of T_2 for the plasma and the water samples. From the information in References (10) and (11), it was concluded that the values of T_2 (T_{21} and T_{22}) were not related to the percent oxygenation, as much as the values of T_1 were. In none of the references and in none of the Bibliography for NMR in Blood was there any data on the relationship between T_1 and percent oxygenation in blood. Because it was chosen in this program to use only oxygenated blood (according to color), deoxygenated blood (according to color), and nitrogenated blood, but no measurements of blood oxygenation, graphs of T_1 versus percent oxyhemoglobin could not be made. The values of T_2 for the various conditions of each blood sample, however, could be compared to the graphs of T_2 versus percent oxyhemoglobin given in References 10 and 11 and reproduced in Figure 10. The first comparison of the T_2 values for arterial blood, blood with non-flowing oxygen bubbles, venous blood and blood with non-flowing nitrogen bubbles is given in Figure 19. The arterial blood has the highest value of T_2 which means it has the highest percent oxyhemoglobin value of 81%. Blood with oxygen bubbles has a value of T_2 less than for arterial blood which means that the oxygen bubbles in blood gave a lower percent oxyhemoglobin (74%) than arterial blood (81%). Venous blood gave a T_2 value of around 76 milliseconds which gives a value of 60% oxyhemoglobin which is much lower than the values for arterial blood and blood with oxygen bubbles. The lowest value of T_2 in Figure 19 is 70 milliseconds for nitrogen bubbled blood which is equivalent to 55% oxyhemoglobin.

The graph in Figure 20 is for the mean values of blood with flowing oxygen bubbles, flowing nitrogen bubbles, and non-flowing bubbles in the blood of air, expired air oxygen, and nitrogen. Included in each category are the values for the tonometered conditions. These values, shown as dotted lines, lead to the conclusion that the T_2 values for the blood with flowing bubbles are much longer than for the condition of no-flow. This means that for in vivo measurements it will be necessary to process the NMR signal so that not only the value of T_2 is determined, but also the blood and bubble flow rates are measured so

that the T_2 measurements can be corrected for the flow of the bubbles to obtain a no-flow value for T_2 from which an accurate value of percent oxyhemoglobin can be determined. SwRI has several years of experience processing NMR signals from flowing coal, where the flow rate for the coal can be determined but at the same time, the total hydrogen signal from the hydrogen can be deconvoluted into the water in the coal and the volatile components of the coal.

The graph in Figure 20 should also have a dotted line for a fifth gas condition - that of degassed blood at T_2 = 155 milliseconds. This dotted line was not shown for clarity.

The last data to be collected is shown in Figures 2 and 22. The bursa which contains the synovial fluid is very evident in the four sagittal NMR images. The arrows are pointing to the squares which define the area in which the values of T_1 and T_2 are determined and are printed in the data column along the left of each image. The procedure used only gives the longest value of T_1 and T_2. The NMR imager cannot calculate multiple values. The values of T_1 and T_2 for the synovial fluid are listed in Table V and the magnitudes of T_1 and T_2, with $T_1 > T_2$, indicate that the synovial fluid is quite viscuous.

In summary then, the following has been concluded.

1. All of the proposed NMR measurements were completed.

2. In blood there is only one value of T_2, but two values of T_1 (T_{11} and T_{12}). *In blood plasma, there is only one value of* T_1 and one value for T_2.

3. The two values of T_1 (T_{11} and T_{12}) do not appear to vary with percent oxyhemoglobin while the value of T_2 does a shown by the graphs in Figures 10, 19, and 20.

4. When the bubbles in the blood are flowing, the value of T_2 increased significantly over the value of T_2 without bubble flow at the same percent oxyhemoglobin. This means that the NMR signal should be processed to determine blood flow rate and bubble flow rate so that the values of T_2 can be corrected to the zero flow values in Figure 10.

5. The evidence to date gives one value for T_1 and one value for T_2 in synovial fluid in vivo.

6. The MRI images of the knee (sagittal) showed very clearly the sacs containing the synovial fluid and it is concluded that an NMR device could be made to measure the values of T_1 and T_2 in vivo in the synovial fluid.

7. The NMR measurements in the blood samples indicate that the values of T_2 are significantly different for oxygenated blood without oxygen bubbles and for oxygenated blood with oxygen bubbles.

8. The NMR measurements from the blood sample indicate that the value of T_2 for venous blood, for nitrogenated blood and for blood with nitrogen bubbles are all significantly lower than the values of T_2 for oxygenated blood both with an without bubbles.

From the above conclusions it can be finally stated that NMR measurements can indicate the presence of nitrogen and oxygen bubbles in the blood in high concentrations when the bubbles are fixed or flowing. The results also indicate that further NMR measurements should be made on blood samples with better control of the basic characteristics of blood such as Ph, water concentration, and plasma concentration. It will also be necessary to measure the percent oxyhemoglobin by other clinical methods so that graphs of T_2 versus percent oxyhemoglobin can be obtained for all of the conditions of gas concentration and gas flow. The following paragraphs will describe briefly the recommended follow-on program.

B. Recommendations

From the results from this program it has been concluded that an NMR measurement of the value of T_2 in blood can be used to indicate the presence of stationary and flowing bubbles of nitrogen and oxygen in the blood. No NMR measurements except the NMR images could be made in synovial fluids because a source for this body fluid was not found during the program. It was found that there were significant differences in the values of T_2, T_{11}, and T_{12} for different samples of blood obtained from different blood sources. Therefore, in the follow-on program it will be necessary to measure and carefully control the basic characteristics of the blood samples when they are received and while they are being measured in the NMR spectrometer. It will also be helpful to determine the effect of heparin on the values of T_{11}, T_{12}, and T_2 and the basic blood characteristics. Southwest Research now has the facilities to determine the basic blood characteristics as well as the percent oxyhemoglobin. These facilities were not available during the program. It will also be necessary to determine the percent oxyhemoglobin in the blood sample while it is in the NMR detection coil.

It is recommended that the following tasks be accomplished during the follow-on program.

1. Redesign and reconstruct the bubble generator and the NMR detection head so that not only the NMR measurements but also determinations of the percent oxyhemoglobin, Ph and other basic blood characteristics can be made.

2. Determine the effects on T_{11}, T_{12}, and T_2 of the treatments such as the addition of heparin given to blood used in sources such as blood banks relative to freshly drawn blood so that more useful blood samples can be obtained.

3. Make the NMR measurements of T_{11}, T_{12}, and T_2 using the modified NMR detection head as described in 1 above, using the samples described in 2 above, for the conditions of oxygen bubbles, nitrogen bubbles, air bubbles, and expired-al bubbles, both with and without a flowing of the bubbles. Not only the NMR determinations but also measurements of the

basic blood characteristics and the flow rate of the bubbles should be made simultaneously. When the results from the above three tasks have produced graphs of T_{11}, T_{12}, and T_2, as a function of percent hemoglobin for all of the conditions of oxygen, nitrogen, and air bubbles (from air and expired air), the follow-on program can proceed to in vivo determinations.

4. To make in vivo measurements in blood, synovial fluid and tissue, a new NMR detection head must be designed and constructed along the lines of the drawings in Figures 6, 7, 8, 11, 12, and 13. When these modifications are designed and added to the SwRI laboratory NMR equipment, then in vivo blood measurements can be made on either animals or human volunteers. The best and most available models will be chosen during a meeting between the sponsor and the SwRI program personnel.

5. Using the modified SwRI NMR spectrometer, measurements of T_{11}, T_{12}, and T_2 will be made in vivo on the blood in the veins and arteries, in the synovial fluids in the joints and in the tissues of the specimens chosen. It is considered that there may be several additional modifications to the NMR equipment which will be found necessary during the NMR measurements which will cause several repetitions of the measurement-modify-measurement cycle until the equipment and methodology are finalized.

6. The data and analysis resulting from the above tasks will permit a preliminary design of the hydrogen transient NM equipment and methodology which can be used to measure the onset of decompression bubbles. The results from Tasks through 5 above will also permit a close estimate of the cost o the detailed design, construction, and test of the equipment for the in-vivo detection of decompression bubbles.

REFERENCES

1. Fukushima, E. and Roeder, S.W., "Experimental Pulse NMR," Addison-Wesley Publishing Co. (1981).

2. Martin, M.L., Delpuech, J.J., and Martin, G.J., "Practical NMR Spectroscopy," Heyden and Son Ltd., (1980).

3. Goldman, M., "Spin Temperature and Nuclear Magnetic Resonance in Solids," Oxford (1970).

4. Bloembergen, N., "Nuclear Magnetic Relaxation," W.A. Benjamin, Inc. (1961).

5. Caspers, W.J., "Theory of Spin Relaxation," Interscience Publishers, (1964).

6. Chiarotti, G., et al., "Proton Relaxation in Pure Liquids and in Liquids Containing Paramagnetic Gases in Solution," Il Nuov Cimento, Vol. 1, No. 5 (1955) p. 863.

7. Brooks, R.A., et al., "Nuclear Magnetic Resonance in Blood," IEEE Trans. on Biomed, Engr., Vol. BME-22 (Jan. 1975), pp. 12-18.

8. Newman, T.S., Hall, D.D., and Linaweaver, P.C., "Gas Phase Separation During Decompression in Man: Ultrasonic Monitoring," Undersea Biomed. Research Vol. 3 (1976) pp. 121-130.

9. Adams, J.D., Olson, R.M., Dixon, G.A., and Burton, R.R., "Ultrasonics in Decompression Sickness Prevention," Proceedings of the 2nd Southern Biomed. Engr. Conf.,"Biomedical Engineering II, Recent Developments," ed. by C.W. Hall, Pergamon Press, New York (1983), pp. 301-304.

10. Thulborn, K.R., et al., "Rapid Measurement of Blood Oxygenation and Flow by High-Field H.NMR," Biochem. Soc. Trans., Vol. 9, 1981, pp. 233-34.

11. Thulborn, K.R. and Radda, G.K., "Correlation of Oxygen Consumption with Energy Metabolism by In Vivo Nuclear Magnetic Resonance"," J. Cerebral Blood Flow and Metabolism, Vol. 1, Suppl. 1 1981, pp. 582-583.

12. Finnie, M., Fullerton, G.D., and Cameron, I.L., "Molecular Masking of the Paramagnetic Effect of Iron on the Proton Spi-Lattice (T) Relaxation Time in Blood and Blood Clots, Maganetic Resonance Imaging, Vol. 4, (1986), pp. 305-310.

13. Jones, D.W. and Child, T.F., "NMR in Flowing Systems," Advances in Magnetic Resonance, Edited by J.S. Waugh, Vol. 8, (1976) Academic Press, pp. 123-148.

14. Gray, Henry, "Anatomy of the Human Body," Edited by W. H. Lewis, Published by Lea and Febiger, Philadelphia (1942).

BIBLIOGRAPHY IN DECOMPRESSION SICKNESS

Assembled by
William L. Rollwitz

1. Olson, R.M., Adams, J.D., Fitzpatrick, E.L., and Burton, R.R., "Intravascular Bubble Formation and the Prediction of Bends" Aerospace Medical Assoc. Preprints, 53rd Annua Scientific Meeting (1983) pp. 122-123.

2. Olson, R.M., Fitzpatrick, and Koegel, E., "Noninvasive Measurements of Human Right Intraventricular Blood Velocity by an Ultrasonic Technique," Am. J. Cardiology, Vol. 49, (1982), pp 1711-1718.

3. Adams, J.D., Olson, K.M., and Dixon, G.A., "The Use of Doppler Precordial Bubble Detector in Altitude Decompressions," Aerospace Medical Assoc. Preprints, 50th Annual Scientific Meeting, (1979), pp. 260-261.

4. Adams, J.D., Olson, K.M., and Dixon, G.A., "Ultrasonic Monitoring of Altitude Decompression," Aerospace Medical Assoc Reprints, 49th Annual Scientific Meeting, (1978), pp. 105-106.

5. Newman, T.S., Hall, D.D., and Linaweaver, P.C., "Gas Phase Separation During Decompression in Man: Ultrasonic Monitoring," Undersea Biomedical Research, Vol. 3, (1976), pp. 121-130.

6. Spencer, M.P. and Johanson, D.C., "Investigation of New Principles for Human Decompression Schedules Using the Dopple Ultrasonic Blood Bubble Detector," ONR Contract Report No. N00014-73--0094, 23 July 1974.

7. Spencer, M.P. and Clark, H.F., "Precordial Monitoring of Pulmonary Gas Embolism and Decompression Bubbles," Aerospac Medicine, Vol. 43, (1972), pp. 762-797.

8. McIver, R.G. and Leverett, S.D., Jr., "Studies in Decompression Sickness," School of Aerospace Medicine Report No SAM-TDR-63-94, (1963).

9. Harvey, E.N., et al, "Bubble Formation in Animals II. Gas Nuclei and Their Distribution in Blood and Tissue," J. of Cellular and Comparative Physiology Vol. 24 (1944), pp. 1-46.

BIBLIOGRAPHY FOR NMR IN BLOOD

1. Barth, K., et al, "Flow Measurement by Magnetic Resonance Imaging," Proc. SPIE Int. Soc. Opt. Engr., Vol. 535 (1985), pp. 26-267.

2. Wehrli, F.W., et al, "MR Imaging of Venous and Arterial Flow by a Selective Saturation - Recovery Spin Echo (SSRSE) Method," J. Computer Assisted Tomogr., Vol. 9, No. 3 (1985), pp. 537-545.

3. Bradley, W.G. and Waluch, V., "Blood Flow: Magnetic Resonance Imaging," Radiology, Vol. 154, No. 2 (1985), pp. 443-450.

4. Koivula, A., et al., "The Effect of Red Cell Concentration and Osmotic Pressure of Solvent on the Nuclear Magnetic Relaxation in Red Cell Suspensions," Proc. of the XIX Annual Conference o the Finnish Physical Soc., Report No. 104 (1985).

5. Yilmaz, A., et al, "NMR Relaxation Mechanism in Serum From Healthy Subjects," XXII Congress Ampere on Magnetic Resonance and Related Phenomena Proceedings, (1984), pp. 483-484.

6. Feinberg, D.A., et al, Pulsatile Blood Velocity in Human Arteries Displayed by Magnetic Resonance Imaging," Radiology Vol. 153, No. 1 (1984), pp. 177-180.

7. Bryant, D.J., et al, "Measurement of Flow with NMR Imaging Using a Gradient Pulse and Phase Difference Technique," J Computer Assisted Tomography, Vol. 8, No. 4 (1984), pp. 588-593.

8. Beall, P.T., et al, "The Systemic Effect of Cancers on Human Sera Proton NMR Relaxation Times," ..agnetic Resonance Imagin (G.B.) Vol. 2, No. 2 (1984), pp. 83-87.

9. Levshi, P.A., et al, "Potential Applications of NMR in Cardiology," Proceedings of the Physical Techniques in Cardiologica Imaging, (8-9 July 1982), Printed 1983, pp. 205-210, (ISBN-0-8527-750-0).

10. Friedman, G.B., "NMR and ESR Studies Related to Blood," Magn. Resonance Review (GB), Vol. 8, No. 3 (1983), pp. 243-282.

11. Revokatov, O.P., et al, "NMR Relaxation in Human Blood Serum and Diagnosis of Malignant Neoplasma," Biophysics (G.B. Vol. 27, No. 2 (1982), pp. 348-350.

12. Kiovula, A., et al, "The Spin-Lattice Relaxation Time in the Blood of Healthy Subjects and Patients with Malignant Bloo Disease," Phys. Med. and Biol. (GB), Vol. 27, No. 7 (1982), pp. 93-947.

13. Burt, C.T., et al., "Nuclear Magnetic Resonance Studies on Circulating Blood "J. Magn. Reson. (USA), Vol. 46, No. 1 (1982) pp. 176-179.

14. Battocletti, J.H. and Halback, R.E., "A Nuclear Magnetic Resonance Non-Invasive Leg Blood Flowmeter," IEEE Frontiers in Engineering in Health Care Conference, 19-21 Sept. 1981, Houston, TX USA.

15. Friedman, G.B. and Sandhu, H.S., "NMR in Blood," Magnetic Resonance Review (BG), Vol. 6, No. 4 (1981), pp. 247-307.

16. Radda, G.K., et al, "A Simple Method of Flow Measurement by Pulsed NMR," J. Magn. Resonance (USA), Vol. 42, No. 3 (1982), pp 488-490.

17. Halback, R.E., et al, "The NMR Blood Flowmeter Design," Med. Phys. (USE), Vol. 8, No. 4 (1981), pp. 452-458.

18. Salles-Cunha, S.X., et al, "The NMR Blood Flowmeter Applications," Med. Phys., Vol. 8, No. 4 (1981), pp. 452-458.

19. Battocletti, J.H., et al, "The NMR Blood Flowmeter Theory and History," Med. Phys. (USA), (1981), pp. 435-443.

20. Halback, R.E., et al., "Blood Flow Detection Using the Flat Cross-Coil Nuclear Magnetic Resonance Flowmeter," IEEE-Trans Biomed, Engr. (USA), Vol. BME-28, No. 1 (1981), pp. 40-42.

21. Sandhu, H.S. Friedmann, G.B., "NMR T Relaxation Time Studies in Normal and Pathalogic Blood," J. CLin. Engr. (USA), Vol. (1979), pp. 357-362.

22. Hochmann, J. and Kellerhals, H., "Proton NMR on Deoxyhemoglobin. Use of Modified DEFT Technique," J. Magn. Resonance (USA) Vol. 38, No. 1 (1980), pp. 23-39.

23. McLacklan, L.A., "Cancer-Induced Decrease in Human Plasma Proton NMR Relaxation Rates," Phys. Med. and Biol. (GB), Vol. 25 No. 2 (1980), pp. 309-315.

24. Battocletti, J.H., et al., "Flat Crossed-Coil Detector for Blood Flow Measurement Using Nuclear Magnetic Resonance," Med and Biol. Engr. and Comput. (GB), Vol. 17, No. 2, (1970), pp. 183-191.

25. Halback, R.E., et al, "Cylindrical Crossed-Coil NMR Limb Blood Flow-meter," Rev. Sci. Instrum. (USA), Vol. 50, No. 4 (1979), pp. 428-434.

26. Eisenstadt, M. and Fabry, M.E., "NMR Relaxation of the Hemoglobin-Water Proton Spin-System in Red Blood Cells," J. Magn. Resonance (USA), Vol. 29, No. 3 (1978), pp. 591-597.

27. Ekstrand, K.E., et al., "Proton NMR Relaxation Times in the Peripheral Blood of Cancer Patients," Phys. Med. and Biol. (G.B.) Vol. 22, No. 5 (1977), pp. 925-931.

* U. S. GOVERNMENT PRINTING OFFICE: 1990--761-051/20091